



# HHS Public Access

Author manuscript

*Adv Mater.* Author manuscript; available in PMC 2022 November 01.

Published in final edited form as:

*Adv Mater.* 2021 November ; 33(46): e2006600. doi:10.1002/adma.202006600.

## Programmable mechanically active hydrogel-based materials

Yixiao Dong<sup>†</sup>,

Department of Chemistry, Emory University, Atlanta, GA, United States, 30322

Allison N. Ramey-Ward<sup>†</sup>,

Wallace H. Coulter Department of Biomedical Engineering, Georgia Institute of Technology/  
Emory University, Atlanta, GA, United States

Khalid Salaita<sup>\*</sup>

Department of Chemistry, Emory University, Atlanta, GA, United States, 30322

### Abstract

Programmable mechanically active materials (MAMs) are defined as materials that can sense and transduce external stimuli into mechanical outputs or conversely that can detect mechanical stimuli and respond through an optical change or other change in the appearance of the material. Programmable MAMs are a subset of responsive materials and offer potential in next generation robotics and smart systems. This review specifically focuses on hydrogel-based MAMs because of their mechanical compliance, programmability, biocompatibility and cost-efficiency. The review first discusses the composition of hydrogel MAMs along with the top-down and bottom-up approaches used for programming these materials. Next, we discuss the fundamental principles for engineering responsivity in MAMS which includes optical, thermal, magnetic, electrical, chemical, and mechanical stimuli. We compare some advantages and disadvantages of different responsivities. Then, to conclude, we summarize the emerging applications of hydrogel-based MAMs from recently published literature, as well as the future outlook of MAM studies.

### Keywords

mechanical active materials; programmable hydrogel actuator; artificial muscle; force sensor; smart skin

## 1. Introduction

In nature, there are numerous examples of how programmed mechanical forces help organisms adapt to their environment. *Mimosa pudica* folds its leaves inwards upon touching or shaking as a defense mechanism<sup>[1]</sup>, caterpillars use waves of deformation to move<sup>[2]</sup>, and the Venus flytrap closes its trapping leaves in response to the minute force of an insect landing on it<sup>[3]</sup>. Hydrogel-based mechanically active materials (MAMs)—also called

\*k.salaita@emory.edu .

<sup>†</sup>These authors contribute equally to this paper

Conflict of interest

The authors declare no conflict of interest.

artificial muscle, actuators, or force sensing materials—can either generate mechanical force or respond to mechanical force, and have been heavily inspired by nature. By definition, hydrogel-based MAMs respond to mechanical inputs or alternatively generate a mechanical output upon receiving an input signal. Other responsive materials or systems that fail to incorporate a mechanical signal will not be discussed and are not considered MAMs.

Hydrogel-based MAMs are the most diverse and intensely studied, and have potential to be programmed with various responding behaviors and have broad applications in areas ranging from biomedical engineering to robotics. Hydrogel programmability, in some literature, refers to the fine-tuning of hydrogel deformation patterns<sup>[4]</sup>. Other works define programmability of hydrogels as molecular sequencing or arrangement within gel networks<sup>[5]</sup>. To provide a more consistent overview of programmable hydrogel-based MAMs, this review defines programmability as the ability to tune the input-output response function of the MAMs through either molecular design or patterning of the material across multiple length scales. There are MAMs that are responsive but the response function cannot be easily altered or tuned. For example, a conventional hydrogel that can swell and deswell by controlling the humidity. But without spatially patterning the material or without doping certain copolymers into the gel, this type of conventional material is not inherently programmable. We will further discuss the approaches to integrate programmability into MAMs in section 3.

In this review, we first describe the chemical components of hydrogel-based MAMs and their fabrication, followed by specific approaches towards programmability. Then, a detailed classification of responsivity mechanisms is provided, along with discussion of the intimate relationships between material structure and their responsive behaviors. We then end by summarizing current applications of MAMs across multiple disciplines, and the future directions and applications of mechanically responsive hydrogels.

## 2. Components of Hydrogels

Mechanical responsivity has been observed in nearly all types of materials both hard and soft materials, spanning from metals to ceramics and polymers. Popular examples include shape-memory metal alloy<sup>[6]</sup>, piezoelectric ceramics<sup>[7]</sup>, thermoresponsive polymers<sup>[8]</sup>. However, this review will exclusively discuss programmable MAMs that are hydrogels or composites primarily comprised of hydrogel polymers. Hydrogel materials are great candidates for flexible devices and bio-engineering studies, and this has inspired multi-disciplinary research and numerous potential applications. To be more consistent, inorganic nanoparticles, plastic, rubber, ceramics, polymer micelles/capsules, will not be discussed in this review since these types of materials are not hydrogels.

Hydrogels are defined as hydrophilic polymer networks—synthetic, naturally derived, or a composite of the two—which can swell and retain water within their volume<sup>[9]</sup>. As such, most hydrogels are considered intrinsically mechanically responsive to hydration stimuli, creating strain by swelling and deswelling, dependent on available water. Moreover, many hydrogels also respond to other external stimuli (detailed in Section 4 of this review), thus offering versatility in the types of triggers that generate a mechanical response. Hydrogels

are highly tailorable and procedures to decorate these polymers with diverse chemical modifications have been reported, hence offering a wide range of applications in industrial, medical, and research arenas. Some examples of polymers used in MAM synthesis are shown in Figure 1.

Though there are many benefits of hydrogel materials, they are subject to distinct limitations. Notably, responsive hydrogels must be kept in a wet or humid environment to maintain their characteristic high water content. Though humidity levels can be leveraged as a way to trigger a mechanical deformation in a hydrogel material (as discussed later in Section 4), in general removing moisture deswells a hydrogel, removing its ability to deform and respond. Despite sensitivity to ambient humidity, hydrogel MAMs remain versatile, programmable materials that are of great interest to scientists in many fields.

Synthetic hydrogels, and synthetic polymers in general, are often selected for their ease of availability, as well as their ability to be chemically modified for unique applications<sup>[10]</sup>. This is especially true of MAMs, where the ability to manipulate chemical and mechanical properties allows for diverse applications and tuned responsiveness. Synthetic polymers can be intrinsically responsive to external stimuli, such as the responsivity of N-isopropylacrylamide (NIPAm) and N-isopropylmethacrylamide (NIPMAm) to heating<sup>[11]</sup>, or the sensitivity of polyethylene glycol (PEG) hydrogels to humidity<sup>[12]</sup>.

Programmable MAMs can also be made entirely or partially of naturally derived materials. While these types of polymers can be subject to sourcing concerns, naturally derived materials offer distinct advantages. Polymers such as alginate, chitosan, and hyaluronic acid are highly sensitive to the ionic strength and the electrochemical environment of their medium<sup>[13]</sup>. Thus, naturally derived materials will generally actuate based on cation content and pH<sup>[14]</sup>. Nucleic acids, long studied for their role in information carrying functions in biology and genetics, can be synthesized and controlled precisely have recently emerged as a biopolymer building block for the construction of responsive hydrogels<sup>[15]</sup>. These gels are sensitive to their thermal and chemical environment, which can alter force production by disrupting hybridization<sup>[16]</sup>.

While some hydrogels are responsive in their pure form, mechanical activity is often induced in gels with the addition of dopants, such as metal nanoparticles or chemical impurities.<sup>[17]</sup> Additionally, multiple synthetic and/or naturally derived polymers can be combined to form composites that leverage the advantages of both materials, enhancing factors such as programmability, responsivity, and material properties<sup>[18]</sup>. Several examples of hydrogel-based MAMs are shown in Table 1, we compare these MAMs based on their responsivity, modulus, and actuation magnitude.

### 3. Programming MAMs

In order to create a dynamic mechanically active material, one needs to be able to program an input-output function where either the input or the output is mechanical. Moreover, the direction of the mechanical response and hence the geometry and shape of the MAM is highly important to achieve useful mechanical work for specific applications. The following

sections describe two general strategies to program MAMs such that the material displays mechanical activity and also such that this activity is most useful.

### 3.1 Bottom-up patterning: Encoding mechanically active hydrogel materials through self-assembly

“Bottom-up” is used to describe a synthetic methodology that stresses the fundamental molecular design of a material, to control its organization and hence control its mechanical functions. Bottom-up molecular programmability is often used for patterning hydrogel materials comprised of DNA<sup>[19]</sup>, peptides<sup>[20]</sup>, synthetic copolymers<sup>[21]</sup>, and polysaccharides<sup>[22]</sup>. Controlling the molecular sequence of these polymer building blocks allows for generating diverse responsivities and mechanical behaviors of MAMs.<sup>[19–22]</sup>

The self-assembly of DNA and peptides has been well-studied for many decades and this fundamental insight is being used to program the self-assembly of various MAMs. For example, Cangialosi et al. generated DNA-acrylamide hydrogels that can be programmed to swell and collapse in response to specific DNA inputs.<sup>[23]</sup> The strategy employed the well-studied hybridization chain reaction to increase the physical length of double strand DNA crosslinkers. The mechanism of actuation will be discussed further in section 4.3. Another example of DNA-hydrogel MAMs were constructed using rolling circle amplification by Merindol et al. to generate force sensing DNA gels<sup>[24]</sup>. An example of peptide-based MAMs is reported by Xue et al.<sup>[25]</sup> in which a peptide supramolecular hydrogel based actuator can be formed in buffer with self-assembly. These cases demonstrate that the self-assembly can affect the structure and function of the MAM, such as the kinetics and the amplitude of the response.<sup>[24]</sup>

In contrast to biologically derived protein and nucleic acid polymers, synthetic polymers are artificial materials that can be controlled during MAM synthesis to program the responsivity of the material. For example, our lab generated core-shell MAMs that are comprised of a gold nanorod core surrounded by a responsive hydrogel shell. The hydrogel shell itself incorporated reactive groups in the outer layer of the material and this was synthesized by adding the reactive monomer at a final stage of the polymer synthesis. In this way, the MAM was programmed with a specific size and composition and this allows for highly uniform application of forces and uniform response to thermal inputs<sup>[26]</sup>. The programmability of MAMs can also be encoded using synthetic copolymers derived from both types of functional segments and the ratio between different segments in the copolymers<sup>[4a, 27]</sup>. For example, Zheng use poly(acrylic acid-co-N-isopropyl acrylamide) as the responsive component of MAMs. By adjusting the ratio between P(AAc-co-NIPAm) and P(AAc-coAAm), the response of MAMs to concentrated saline solution was fine-tuned<sup>[4a]</sup>. However, in comparison with the synthesis of bio-macromolecules, synthetic copolymers are less controllable in monomer sequence but more accessible in regards to low cost and facile synthesis. Further details of MAM programmability will be introduced in later sections.

The precision of bottom-up molecular assembly is ultimately superior in terms of controlling the nanoscale organization of materials. However, at larger length scales (greater than 1 micron) there are not many examples of materials that can be organized using self-assembly at this length scale. Hence this represents one of the limitations of bottom-up based

self-assembly and motivates the work using top-down methods for fabrication. Another consideration is the relatively high cost and low yield associated with nucleic acid and peptide-based hydrogel materials in comparison to synthetic polymers that lack sophisticated self-assembly programming.

### 3.2 Top-down patterning: Tailoring hydrogel architectures into 3D geometries across multiple length scales

In contrast to bottom-up self-assembly, “top-down” approaches tend to be more labor-intensive creating structures in a more serial process but providing highly tailored geometries and configurations for MAMs.<sup>[28]</sup> These top-down approaches confer responsivity beyond the molecular structure and properties of the material, leading to an architecturally-directed responsivity. Indeed, controlling the size and geometry of a responsive material is a well-reported mechanism for programming MAMs. This is exemplified by the works of Ye et al., demonstrating that the thickness and aspect ratio of silk fibroin-based hydrogel nanosheets controls their internal stress production and ultimate deformation under a specific stimulus<sup>[29]</sup>. The size, shape and composition of a MAM can also adjust its speed of actuation (Table 1). In general, smaller structures are able to respond more rapidly than larger ones<sup>[30]</sup> due to the ability to more rapidly move water out of the hydrogel to induce deswelling<sup>[31]</sup>. Such parameters can be easily controlled using top-down fabrication.

Some common “top-down” approaches that program responsive architectures are molding, lithography, 3D printing, electro-spinning, and gradient control (Figure 2). Although “top-down” and “bottom-up” approaches are distinct and separate concepts in MAM programming, they are not exclusive to each other. In fact, it is quite common that programmable MAMs include both methods to better achieve the desired response, composition, and form.<sup>[32]</sup> Nonetheless, the following section describe methods to achieve top-down patterning of MAMs.

**3.2.1 Molding**—As perhaps one of the most accessible “top-down” programming methods, molding has been widely adopted to direct the higher-level architectural design of MAMs<sup>[33]</sup>. Molding can be achieved through two mechanisms: casting and forming the hydrogel inside a pre-fabricated mold, or cutting a piece of bulk hydrogel down to the desired shape and size. Molding is also a low-cost hydrogel fabrication method, making it optimal for initial proof of concept testing, as well as large-scale production of such materials. Also, the materials to fabricate molds can be rather versatile, such as glass, PDMS, and polymer resin, which can be selected to better accommodate the hydrogel synthesis. For example, our group used Delrin® mold to fabricate MAMs with required hydrogel patterns to create smart skin MAMs.<sup>[34]</sup> The two main advantages of molding—cost efficiency and diverse options—make molding very common for the fabrication of programmable MAMs.

Nevertheless, it is important to note that molding technologies are limited to micron-size resolution in MAM fabrication. For smaller sized MAMs, traditional molding technology lacks the required spatial resolution. Moreover, as-molded MAMs are generally 2D rather

than more sophisticated 3D structures. These disadvantages limit some of the applications of MAMs generated using molding technologies.

**3.2.2 Photolithography**—Photolithography is a patterning technology that uses a patterned light source to control the formation of a photosensitive polymer, leaving a latent image in the polymer substrate that can be later revealed by dissolving or washing away the unpolymerized precursor<sup>[35]</sup>. In contrast to traditional molding methods, photolithography provides higher spatial resolution that has recently been extended to the sub-50 nm length scale. Generally, photolithography for fabricating programmable MAMs can be divided into two types: masked and maskless. For masked photolithography, as the name suggests, a photomask designed with a negative of the desired shape and size is required to shade parts of the precursor solution and only polymerize parts of the MAM in a specific pattern. Shim et al. <sup>[36]</sup> reported the photolithography fabrication of tunable microcapsules based on dual UV exposure with masks, in which case the bending response of these MAMs is mainly dictated through the pattern-shape transferred by the photomask.

In contrast, maskless photolithography is the patterning of MAMs by physically controlling the location of the polymerizing light source, i.e. moving a laser beam. One example of this technique is found in the work of Martella et al.<sup>[37]</sup>, where a “micro-hand” MAM that can grasp micron-sized objects was fabricated via a pre-programmed laser beam that selectively cured the hand shape into a precursor solution.

Both masked and maskless photolithography have their own advantages and disadvantages towards programmable MAMs design. For fabrication of large-scale MAMs, or production of many identical structures, mask-type photolithography is more efficient, as one mask can be used for the construction of hundreds of MAMs. However, maskless photolithography is more flexible for rapid, on-demand fabrication of multiple different designs, bypassing the need for a new mask to be created for each change in pattern.

In comparison with other programming technologies, photolithography provides a high degree of spatial control. However, the samples produced by photolithography are typically very thin, which has limited 3D applications. Nonetheless, the use of photomasks can precisely tune the architecture of a MAM to create complex geometries upon stimulation. One example of such work introduces holes of varying size and number into thin hydrogel structures. This created areas of stress concentration within the film, transforming its response from a simple change in curvature to a complex, multi-step folding into precisely designed 3D shapes<sup>[33c]</sup>. Such rationally designed photomasking strategies, in combination with novel techniques such as layer-by-layer photolithography, provide methods to overcome the initial limitations of this technique, though it generally increases the time and complexity of the protocol.

**3.2.3 3D printing**—Another method for creating complex material architectures is additive manufacturing techniques such as 3D printing, which has found cutting edge applications in biomedical sciences, electronics, and aerospace engineering<sup>[38]</sup>. In most work, 3D printing is defined as a technology that produces physical objects through layer-by-layer deposition of materials, often based on 3D computer-assisted design (CAD)

models.<sup>[39]</sup> Compared with other methods introduced in this review, 3D printing provides structural control on both large and small spatial scales. As a highly tunable method in both size, material, and architecture, 3D printing of hydrogel materials is particularly advantageous for fabricating programmable MAMs. In fact, using 3D printing to create stimuli-responsive structures has been termed “4D printing” to emphasize the extra “dimension” of responsivity<sup>[40]</sup>. Because 4D printed objects are 3D printed objects, and because the term 4D printing is not universally adopted in the field, we will use the two interchangeably in this text.

Zheng et al.<sup>[4a]</sup> reported a type of programmable MAMs produced by 3D printing, in which the hydrogel precursor was fast-crosslinked by carboxyl-Fe<sup>3+</sup> coordination complexes and the bulk gel was knitted by directional hydrogel fibers. 3D printing was used to control the alignment angle of the fibers, which in turn fine-tuned the deformation profile of the material. 3D or 4D printing can also be integrated with other fabrication methods. Odent et al.<sup>[41]</sup> reported a 4D printing technology based on time-resolved photolithography, which the MAMs was produced through layer-by-layer deposition of gel precursors, and each layer in the 3D construct subsequently polymerized into the desired shape via photolithography. The fabrication of MAMs relies on the precise deposition of hydrogel layers with different volume expansion properties, thus provided a general platform to produce multi-responsive MAM systems.

Even though 3D printing provides high spatial control of the geometry of MAMs, several challenges could limit its future applications. First of all, since it produces 3D objects through deposition of a single layer at a time, the complexity of the MAM’s design will limit the efficiency of this method. Additionally, for hydrogel-based materials, 3D printing requires a fast curing mechanism which would limit the material types to those that can be rapidly cured through remotely-controlled process such as photopolymerization. However, as additive manufacturing technologies improve and become more widely available, these challenges may be overcome and open new applications for 3D printed MAMs.

**3.2.4 Electro-spinning**—Electrospinning is a method related to 3D printing that provides a simple and versatile method for generating ultrathin fibers from a rich variety of materials including polymers, composites, and ceramics<sup>[42]</sup>. This method has been extensively studied for potential biomedical applications, such as tissue engineering<sup>[43]</sup>. Electrospinning works to program MAMs by controlling the directionality and alignment of hydrogel fibers, which in turn influences the mechanical properties and directional responsivity of the material. Liu et al.<sup>[44]</sup> reported the fabrication of a two layered MAM with oriented hydrogel fibers through electro-spinning. The MAM naturally bends at different temperatures, due to the temperature responsive behavior of an interwoven pNIPAM layer.

Electro-spinning is a facile method to produce programmable MAMs. However, materials produced by electro-spinning generally requires manual cutting to produce the final sample, as the spinning method creates a wide mat of fibers without a defined shape. It is similar to the molding method in this way, and may not be suitable to produce micron-scale MAMs.

**3.2.5 Gradient manipulation**—The phrase “gradient materials” was originally proposed by Japanese scholars in 1980 to describe a class of engineered materials exhibiting spatially inhomogeneous microstructures and properties.<sup>[45]</sup> Compared to layer-by-layer assembled materials, gradient materials do not have a clear boundary between different layers or phases within the hydrogel. This creates a unique advantage for gradient materials over layer-by-layer assembly, providing continuity between material sections of differing properties. Moreover, gradient materials are usually synthesized with one-step protocols that do not require multi-step layer synthesis and assembly. Luo et al<sup>[46]</sup> introduced a kind of hydrothermal method to synthesize a gradient in porous elastic hydrogels, providing them with programmable locomotion. Due to the differentiation of NIPAM component, the hydrogel bent when heated above the material LCST, and this bending feature was related to the thickness of the hydrogel. After blending with PPy nanoparticles, the hydrogel exhibited programmable locomotion under laser stimulus.

## 4. Responsivity

A hallmark of MAMs is their ability to respond to a variety of external stimuli (Figure 3). These responses are intrinsically tied to the design of the material, and each has unique advantages and disadvantages, dependent on the intended use of the MAM. In the remainder of this review, we will discuss these responsive mechanisms and their emerging applications.

### 4.1 Thermoresponsive Materials

Among the most commonly studied actuating hydrogels are the thermoresponsive polymers, which undergo conformational changes at the molecular level when heated to specific temperatures. This temperature is defined as either a lower critical solution temperature (LCST) or upper critical solution temperature (UCST), as described below.

**4.1.1 LCST MAMs**—MAMs with a lower critical solution temperature (LCST) are hydrogels that become less soluble upon increasing the environmental temperature. This reduced solubility of polymer chains causes the overall hydrogel to shrink or collapse. Poly(N-isopropylacrylamide) (pNIPAM) and its derivatives have been studied intensively many decades because of their facile synthesis and well-characterized LCST that is conveniently above room temperature (~32 °C). By making pNIPAM hydrogels using different monomers or co-polymers and employing a variety of crosslinking approaches, the transition temperature of pNIPAM hydrogels can be tuned which leads to the ability to tune the mechanical force output.

Similar to most hydrogel-based MAMs, in order to acquire programmable bending or actuating, temperature responsive MAMs are typically designed with multiple components that produce an asymmetric response profile. In general, two or more layers of materials with different responsivity may be stacked together, resulting in bending due to the dissimilar mechanical properties of the different layers. Yao et al<sup>[47]</sup> designed such a bilayer MAM based on pNIPAM with nanoclay as a crosslinker. The MAM was made of two layers that were fabricated with different concentrations of nanoclay, which provides each layer with different mechanical properties during temperature-driven deswelling. As a result, the material bends towards the more rigid side, which contain more nanoclay. Interestingly,



during initial heating MAMs displayed a counter-intuitive response where the MAM bent toward the side with less nanoclay but this was due to the mis-matched deswelling kinetics. MAMs that are fabricated with this pNIPAM/nanoclay system eventually demonstrated robust mechanical properties that can easily lift small cargos, such as plastic beads or PTFE blocks, as a result of patterning the material into specific shapes as a claw.

Creating a multi-layer hydrogel system with different mechanical properties is not the only way to fabricate MAMs that generate bending or twisting motions. There are other methods, such as gradient manipulation<sup>[48]</sup>, evaporation<sup>[49]</sup>, and fiber implantation<sup>[50]</sup>, creating programmable MAMs with similar bending behavior. Liu et al.<sup>[48]</sup> developed a facile method to fabricate gradient MAMs by polymerizing N-isopropylacrylamide (NIPAM) monomer with dispersed montmorillonite which is a type of clay. Montmorillonite first formed a gradient dispersion by gravity, after which the NIPAM monomer nucleated around it and began to polymerize. As a result, the hydrogel had a gradient distribution of pNIPAM, with a higher density near the bottom and lower density near the top. Upon thermal stimulation, the MAMs bend towards the side with higher pNIPAM density due to larger actuation forces.

In addition to incorporating anisotropy in MAMs by top down method, like gradient manipulation, anisotropic properties of MAMs can also be formed through bottom up method such as molecular stacking/assembly of liquid crystal molecules<sup>[51]</sup>. Kularatne et al. reported a programmable shape morphing liquid crystal hydrogel by copolymerizing ionic dimethacrylate derivative of perylene-3,4,9,10-tetracarboxylic diimide with pNIPAM<sup>[51]</sup>. The anisotropy of the hydrogel MAMs is based on pre-aligned perylene-3,4,9,10-tetracarboxylic diimide molecules, which can program the deformation of pNIPAM when heated above the LCST. This intrinsic molecular-assembly determined anisotropy provided by liquid crystals inspired a new general approach to manipulate the mechanical responsiveness of thermoresponsive MAMs, and is potentially applicable to others, such as redox, pH, and light responsiveness.

It is worth noting that MAMs that contain pNIPAM or its derivatives are not only sensitive to direct bulk heating. Another approach is to produce “indirect heat” to trigger the LCST response of pNIPAM materials. For example, by incorporating nanomaterials, such as gold nanoparticles, graphene, Fe<sub>3</sub>O<sub>4</sub>, or other light absorbing materials with pNIPAM hydrogels, MAMs could be triggered by “indirect heat” that is transferred through light, electrical, or alternative magnetic field. These are detailed throughout this review as light responsive MAMs or multi-responsive MAMs.

**4.1.2 UCST MAMs**—Hydrogel backbones that have an upper critical solution temperature (UCST) are mostly created through binary polymer networks, in which polymer-polymer hydrogen bond interactions are stronger than polymer-water bonds interactions at room temperature<sup>[17, 52]</sup>. Generally, this kind of polymer-polymer interaction network can be built through two methods: copolymerization, or interpenetration of different polymer networks.

The UCST window and UCST temperature are mainly controlled or fine-tuned by three different aspects: components of polymer-polymer pairs, ratio between the different polymers, ionic strength and pH of aqueous medium. At least three types of polymer-polymer pairs have been reported recently for the fabrication of MAMs. Hua et al.<sup>[53]</sup> reported UCST MAMs based on interpenetrating networks of poly(acrylic acid) (pAAc) and poly(acrylamide) (pAAm). Homogeneous pAAm gel networks were first synthesized by radical polymerization. Then, to create programmability in the design, an anisotropic MAM was fabricated by photopolymerizing the pAAc network on one side of pAAm network. Upon cooling to room temperature, the UCST MAMs bend to the side that is rich in pAAc. The temperature responsivity has a wide window of 30–60 °C, and programmable actuation was realized through partial heating/cooling of specifically designed MAM shapes. Similarly, Auge et al.<sup>[52a]</sup> studied the UCST volume transition of poly(acrylamide-co-acrylonitrile) copolymer hydrogel MAMs, and Ding et al.<sup>[52b]</sup> studied the UCST transition of methyl cellulose-graft-polyacrylamide (MC-g-PAM) hydrogel MAMs.

Due to the fact that acrylamide groups can interact with different ions in the solution, UCST MAMs with acrylamide groups are highly sensitive to the presence of ions, such as  $\text{H}_2\text{PO}_4^-$ ,  $\text{Cl}^-$ ,  $\text{SCN}^-$ , etc.<sup>[53]</sup> This property either opens the door towards more diverse responsive mechanisms, or in some applications limits UCST MAMs use, such as in physiological environments. Compared to UCST MAMs, LCST MAMs are more ion-independent since their volume transition does not rely on interactions between different polymers.

A very specific polymer-polymer interaction, DNA double-strand hybridization, can crosslink or partially crosslink hydrogel MAMs to create UCST-type responsivity based on duplex structure melting temperature. However, DNA related MAMs are also reported as pH responsive, ion-responsive, chemical responsive, or multi-responsive, more so than temperature responsive.

## 4.2 Light Responsive Materials

One of the most common methods of triggering actuation in mechanically active hydrogel materials is via illumination with specific wavelengths of light. The light-driven mechanism offers several advantages: remote actuation, tunable responsiveness, and the potential to use natural sunlight in some applications. The majority of these MAMs are composites, with the inclusion of nanoparticles or specific chemical compounds reacting with the light and driving the response (Figure 4). In this section, we will detail the current mechanisms used to attain actuation in this manner.

**4.2.1 Infrared and Near-Infrared Light**—One mechanism for light-driven hydrogel actuation is responsivity to far red, near-infrared (NIR) and infrared (IR) light. To accomplish this, nanomaterials, such as gold nanostructures, are incorporated into a hydrogel matrix made of thermoresponsive polymers: for example, N-isopropylacrylamide (NIPAM)<sup>[54]</sup>. Noble metal nanostructures found in these composite MAMs exhibit distinct absorption spectra at visible and IR zone of wavelengths that is highly dependent on particle morphology: larger aspect ratios (length/width) show a demonstrated red-shift in absorbed IR wavelengths<sup>[55]</sup>. This causes a surface plasmonic resonance in the nanoparticle,

leading to photothermal heating that drives the local volume phase transition of the thermoresponsive polymer matrix<sup>[26, 56]</sup> (Figure 4a). One example of this technology is the optomechanical actuator (OMA) developed by our group<sup>[26]</sup> where a poly-N-isopropyl methacrylamide (NIPMAm) nanoparticle is polymerized around a gold nanorod core to absorb NIR light. The diameter of these OMAs collapses from ~500 nm to ~250 nm upon illumination, and can be used to apply forces to external systems, such as living cells and biomolecules (Figure 4b)<sup>[26, 57]</sup>.

However, metallic nanoparticles are not the only way to achieve IR responsivity in MAMs. Graphene nanostructures have also been employed, and these provide light-to-heat conversion similar to metals. Graphene, and graphene oxides, undergo photothermal heating under numerous wavelengths, including strong absorption peaks in the IR, due to a strong photoelectric effect<sup>[58]</sup> (Figure 4c). Another interesting property that arises from this effect in graphene-containing MAMs is electrical conductivity (this can also induce mechanical responsivity, as described later in this section). This was leveraged by Shi and colleagues to create a light-responsive electrical switch using a NIPAM and graphene oxide composite (Figure 4d)<sup>[59]</sup>. Other actuating hydrogels utilizing this mechanism have incorporated graphene oxide nanosheets<sup>[60]</sup>, or carbon nanotubes<sup>[61]</sup>.

Other semimetallic structures can provide NIR/IR photothermal conversion in MAMs, though these are less common. Notably, WS<sub>2</sub> nanosheets have been incorporated with hydrogel polymers to drive programmable actuation responses<sup>[62]</sup>.

One of the main advantages of using IR or NIR light for actuating materials is that these wavelengths penetrate many materials. This broadens the locations and scenarios in which actuating hydrogels can be applied. For example, NIR light is known to penetrate biological tissues, opening up the use of actuators in clinical applications. Applications of actuating materials are reviewed in depth in Section 5.

**4.2.2 Ultraviolet Light**—Another class of light-responsive MAMs that are well-studied are the ultraviolet (UV) responsive hydrogels. This mechanism of action here still requires a chromophore with extinction at UV-wavelengths as well as nanomaterials that absorb in this range. Graphene oxide nanoparticles in particular have a strong absorption in the UV range, and can be incorporated into hydrogels to provide thermally triggered actuation as described above.

A commonly used moiety to drive light-to-force conversion is the azobenzene group. When irradiated at 300–400nm, azobenzenes undergo a photo-isomerization that drives the conversion from the ground *trans* state to the excited *cis* state. This physically deforms the molecule (Figure 4e), and may also change its affinity for other molecules to create reversible host-guest interactions<sup>[63]</sup>. One interesting example of a MAM driven using azobenzene photo-isomerization was reported by Takashima et al., where they showed that the interaction between azobenzene and cyclodextrin can be controlled with light, leading to reversible hydrogel actuation<sup>[63b]</sup> (Figure 4f). Another molecule used for photo-mechanical conversion is stilbene, which also undergoes photo-isomerization under UV irradiation and has been demonstrated in MAM systems<sup>[64]</sup>. Interestingly, some of these azobenzene-based

UV responsive materials also respond to longer-wavelengths (> 350 nm), such as blue lasers<sup>[63b]</sup>.

**4.2.3 Visible Light**—Though less common, actuating materials can also be programmed to respond to light at specific visible wavelengths, or to white light. This provides a desirable specificity to the actuating response, whereas many NIR/IR and UV responsive MAMs respond to a broader range of wavelengths. These visible-light responsive MAMs incorporate chromophores and nanomaterials akin to the UV and NIR classes of MAMs. Typically, these MAMs are comprised of composites of thermoresponsive polymers doped with nanoparticles such as gold<sup>[65]</sup>, iron oxide<sup>[34]</sup>, and graphene oxide<sup>[66]</sup>. To the best of our knowledge there are not many examples of MAMs that incorporate photoisomerization using visible light mechanisms to drive actuation. The photothermal heating of a responsive polymer represents the most commonly employed mechanism to generate actuation in hydrogels using visible light and the optomechanical actuator (OMA) particle shown in Figure 4b is a good example. Another unique example of MAMs driven using visible light combines gold nanoparticles with titanium-based nanosheets in a NIPAM matrix. Illumination with blue light ( $\lambda = 445$  nm) drives photothermal heating of the nanomaterials and the shrinking of pNIPAM hydrogel, while the titanate sheets was pre-aligned by strong magnetic field so that overall anisotropic response of pNIPAM hydrogel is established<sup>[67]</sup>. MAMs can also be programmed to respond to white light or even natural sunlight<sup>[34]</sup>, augmenting their usefulness in practical applications, as described below.

Of note, thermally and photothermally responsive materials exemplify the relationship between material size and the time of actuation response (Figure 4g). Zhao and colleagues conducted an analysis of representative publications in this field and found that larger-sized hydrogels require longer times to deswell. Specifically, the time constant of deswelling increases linearly with the square of the particle radius. They also note that optically heating hydrogel particles from the inside, as is the case for the optomechanical actuator particles, leads to a significant enhancement in the rate of deswelling that deviates from bulk heating of hydrogels. Fundamentally, a this relationship arises due to the rate of water movement in and out of the hydrogel system<sup>[68]</sup>. These results emphasize that the geometry of a MAM and its mechanism of responsivity can both be used to program their response.

## 4.3 Chemical responsivity

Chemo-responsive MAMs are a class of actuating material that may respond to one or more of a broad array of chemical inputs. The mechanical response of these MAMs may be triggered by ion concentrations or the presence of a specific molecule, or through more complex means such as enzymatic activity or oxidation-reduction reactions. In this section, we describe the mechanisms involved in each type of chemical responsivity and examples of MAMs designed within this section of the literature.

**4.3.1 pH responsive MAMs**—There are two major types of pH responsive MAMs: proton-donors and proton-acceptors. A majority of proton-donor type MAMs contain carboxyl acid<sup>[69]</sup> as the proton donor. When the environmental pH is less than the pKa of the material, proton-donating groups lose their charge, resulting in deswelling of the hydrogel.

Proton-acceptor type MAMs typically have nitrogen or metal complexes in their functional groups as proton acceptors, such as amines<sup>[69e, 70]</sup>, pyridines<sup>[71]</sup>, Fe<sup>3+</sup>-catechols<sup>[33d]</sup>, and related molecules<sup>[72]</sup>. When the environment is more basic (pH > pKa), proton-*accepting* groups lose the positive charge and cause hydrogel deswelling.

The programmability of pH responsive MAMs can arise from bottom-up assembly or top-down design. For example, Zarzar et al.<sup>[69b]</sup> reported on the role of the architectural design of submerged hydrogel-actuated polymer microstructures (Figure 5a). These substrates with microposts or microfins, were first made by creating a mold in epoxy resin, then copolymerizing acrylic acid and acrylamide to create the pH-responsive structure. Due to the fact that acrylic acid has a pKa of 4.25, the hydrogel contracts at lower pH such that the microstructures are actuated and bend in one direction. All the micropillars bend to one side because the experiment employed unidirectional flow of the buffer within the microfluidic channel.

Another important class of pH responsive MAMs are based on DNA hydrogels. These hydrogels show tunable pH responsivity that is controlled by the nucleic acid sequence. One example is reported by Gibson et al.<sup>[73]</sup>, in which the pH responsive DNA motif is formed by Hoogsteen interactions that form a triplex structure due to the protonation of the cytosine base<sup>[74]</sup>. The formation of the triplex motif mechanically brings two nanoparticles in physical proximity within the hydrogel which results in a shift of the spectra absorbance peak. In another example, it was reported that cytosine-rich domains form interlocking domains (i-motif) when the environmental pH drops to around 5.0<sup>[75]</sup>. Such pH-responsive nucleic acids often incorporate C-rich motifs because the C bases have a pKa ranging from ~4 to ~6 and the protonation can disrupt the conventional Watson-Crick base pairings, and thus the protonated C nucleobases form C<sup>+</sup>-C pairings instead of C-G pairings. This mechanism has inspired work where pH responsive MAMs were created using DNA-crosslinked hydrogels. Guo et al.<sup>[75b]</sup> reported the synthesis of shape memory hydrogel MAMs that are made of DNA-crosslinked polyacrylamide. Two different DNA crosslinkers cooperatively determine the swelling and deswelling states of the hydrogel. The first DNA strand forms crosslinkers at acidic (pH=5.0) conditions due to its cytosine rich sequence that forms an i-motif, while the other oligonucleotide is palindromic and forms crosslinks that non-pH responsive. At higher pH (8.0), the cytosine-rich DNA crosslinker denatures and the gel adopts a quasi-liquid form because of the reduced overall crosslinking density, and thus causing swelling of the hydrogel. However, when the pH is 5.0, the cytosine-rich DNA crosslinker strands are protonated reverting back into interlocking domains (i-motif), and therefore collapsing and recovering its original shape (Figure 5b and c). The interactions between protonated cytosine and other DNA bases provide a distinct toolbox to fabricate pH responsive programmable MAMs.

**4.3.2 Oxidation-reduction responsive MAMs**—Redox (oxidation-reduction reaction) responsive MAMs (RRMAMs) can be triggered by either by reducing/oxidizing reagents<sup>[76]</sup> or alternatively, such MAMs can be triggered using an external electric field<sup>[25]</sup>. Note that electrically triggered MAMs are detailed alongside other electro-responsive MAMs later in this review (Section 4.5.2).

In general, redox reactions cause swelling/deswelling changes in RRMAMs in two ways: altering the intrinsic hydrophilicity (hydration) of redox groups in the hydrogel, and/or by modulating molecular interactions between redox groups and other molecules in the hydrogel. The former aspect can directly change the swelling state through hydrophilicity, while the latter works to change crosslinking density or molecular assembly.

One of the pioneering examples of RRMAMs was developed by Yoshida et al., utilizing the Belousov–Zhabotinsky (BZ) reaction to drive the actuation of RRMAMs<sup>[77]</sup>. BZ reactions are well known for their self-oscillating behavior, in which the catalyst ruthenium tris(2,2'-bipyridine) ( $\text{Ru}(\text{bpy})_3^{2+}$ ) is periodically oxidized into ( $\text{Ru}(\text{bpy})_3^{3+}$ ). In MAMs, the ruthenium complex can be modified, such as with the addition of an alkene group, and then copolymerized with other monomers to make RRMAMs. Due to the fact that ( $\text{Ru}(\text{bpy})_3^{3+}$ ) is more charged than ( $\text{Ru}(\text{bpy})_3^{2+}$ ), the hydrogel follows ion fluxes produced by the BZ reaction to shrink and expand cyclically (Figure 6a). This self-oscillating hydrogel was further programmed with a variety of shapes and asymmetric structures for different applications, such as autonomous mass transportation<sup>[76b, 78]</sup>, artificial cilia<sup>[79]</sup>, and self-walking robots<sup>[80]</sup>.

In addition to hydrophilicity manipulation as a result of redox reactions, the host-guest interaction is another mechanism of actuation in RRMAMs<sup>[76f]</sup>. For example, the host-guest interaction between ferrocene and  $\beta$ -cyclo-dextrin ( $\beta$ CD) is one of the most well studied redox responsive host-guest pairs, where the two molecules associate and dissociate in different redox states, which can be harnessed to create actuation<sup>[76e]</sup>. Nakahata et al.<sup>[76c]</sup> reported a hydrogel MAM crosslinked through ferrocene/ $\beta$ CD pairs. In this system, oxidation of ferrocene caused the dissociation of the ferrocene/ $\beta$ CD pairs, lowering the crosslinking density of the hydrogel and therefore causing the gel to swell (Figure 6b).

Recently, the library of RRMAMs has been further expanded. Novel molecular interactions such as donor-acceptor pairs<sup>[81]</sup> and  $\pi$ -stacking<sup>[76a, 76d]</sup> have been developed and programmed for hydrogel-based RRMAMs. These mechanisms are working to address the slow kinetics and small volume changes exhibited in traditional RRMAMs<sup>[76d]</sup>, to create more significant and on-demand responsivity for future studies and applications.

**4.3.3 Biomolecule responsive MAMs**—Biomolecule sensing and subsequent programmed response are of great interest, particularly in the areas of diagnostics, biological sensing, and drug delivery<sup>[82]</sup>. Biomolecule responsive MAMs (BRMAMs) have been intensively reported over the past few decades, and a variety of responding mechanisms have been developed to detect the target biomolecules for different purposes. These materials generate a mechanical response to a variety of target molecules, such as glucose<sup>[31, 83]</sup>, enzymes<sup>[84]</sup>, and DNA<sup>[23, 85]</sup>, among others<sup>[86]</sup>. In general, the responsivity of these BRMAMs relies on engineering the hydrogel such that it incorporates a specific molecular moiety that generates the response in the hydrogel. This biomolecule interaction typically results in changes of either the crosslinking density or the overall hydration of the hydrogel. In the following paragraphs we describe specific examples that harness this general concept.

Glucose is one of the most well studied target molecules for BRMAMs<sup>[31, 83, 87]</sup>, as the ability to sense and respond to glucose levels has expansive implications, from diabetes research to microbiology. Sim et al.<sup>[83a]</sup> designed a self-helical hydrogel fiber made of a nylon core and hydrogel sheath modified with phenylboronic acid (Figure 7a), which can reversibly form bonds with glucose. Upon increasing the concentration of glucose to 1 M, the molecular complex formed by phenylboronic acid and glucose increases the overall hydrophilicity and water content which leads to swelling of the hydrogel sheath, and producing a maximum tensile strain of 2.3%. Once the glucose concentration drops, the BRMAM can reverse the swelling response and recover its original mechanical properties. This particular hydrogel fiber design also has greater mechanical strength (~1MPa) than other existing glucose responsive hydrogels due to the nylon core. This is just one example of a glucose responsive BRMAM that provides a new strategy for designing materials with greater durability.

Compared with other responsive BRMAMs, enzyme-responsive MAMs rely on the cleavage of specific moieties to modulate crosslinking density and hydration in hydrogel networks. This mechanism of responsivity has remarkably high specificity, but is irreversible. A slightly different example of an enzyme responsive MAM was developed by McDonald et al.<sup>[84a]</sup>. The cleavage of target peptide branches by thermolysin creates a more cationic polymer network, causing swelling (Figure 7b). Importantly, this mechanism is highly enzyme-specific, as the reported gel structures only responded to thermolysin, but not other enzymes such as chymotrypsin. Though the density of branched peptide molecules in this gel system is relatively low, the volumetric change of enzymatic response could reach up to 30%. Athas et al.<sup>[84c]</sup> reported enzyme responsive MAMs with an even greater response amplitude (Figure 7c). In this work, the bulk gel was hybridized by three different “sub-gels” patterned in an asymmetric fashion. The enzyme collagenase specifically degrades the gelatin-based sub-gel at room temperature, creating a mechanical mismatch that caused bending towards the cleavage side.

MAMs that can sense specific DNA oligonucleotide sequences are another class of BRMAM, which have advantages in terms of programmability compared to peptide and protein-based materials. Moreover, building materials with mechanical response to nucleic acid inputs has potential utility in diagnostics. For example, Cangialosi et al.<sup>[23]</sup> designed DNA responsive MAMs with a photopatterned bilayer structure (Figure 7d). The hydrogel was crosslinked by DNA duplexes which triggered a hybridization chain reaction (HCR) in the presence of two specifically designed DNA hairpin targets. The HCR greatly increases the length of the double stranded DNA crosslinkers in the gel, inducing the swelling and actuating of MAMs. Although the responsive kinetics in this system were relative slow and the response was irreversible, the MAM was capable of nearly 100-fold volumetric expansion. To the best of our knowledge, this response represents the greatest volume change reported in a MAM material, and speaks to the large persistence length of double stranded DNA (~50 nm) and its high charge density.

**4.3.4 Humidity responsive MAMs**—All hydrogels are, to some degree, mechanically responsive to changes in hydration state due to their defining high water content. However, some hydrogels are specifically designed to harness or amplify this water responsiveness.

The responsive moieties of humidity-responsive MAMs (HRMAMs) are mostly made of poly(ethylene glycol) (PEG)<sup>[12, 30, 88]</sup> or polyethoxysiloxane<sup>[89]</sup>. Some of these humidity responsive MAMs are quasi-hydrogels, where sensitivity to water is enhanced by reducing the original amount of water contained in the unactuated gel. In comparison to other chemical responsive MAMs, HRMAMs usually have a more rapid response (responding within seconds) and facile synthesis. The latter provides more possibilities for higher-level architectural programming, such as 3D printing<sup>[30, 90]</sup> and electrospinning<sup>[88a]</sup>. Furthermore, since HRMAMs tend to have less water content than common hydrogel MAMs, HRMAMs demonstrate better mechanical performance in their strength, fatigue properties, and locomotive speed<sup>[12, 30, 91]</sup>.

**4.3.5 Ionic strength (IS) responsive MAMs**—Actuation can be achieved in hydrogel-based MAMs by changing the ionic strength (IS) of their environment<sup>[92]</sup>. Theoretically, most polyelectrolyte-based hydrogels are IS responsive, such as poly(acrylic acid)<sup>[93]</sup>, polypeptides<sup>[92]</sup>, and alginate<sup>[14b]</sup>. Generally speaking, the charge shielding effect of high-salt environments leads ionized groups in the hydrogel to have reduced charge repulsion, so that deswelling occurs in the bulk gel. However, only a few existing studies of hydrogel-based MAMs focus solely on IS responsive behavior. Instead, many studies tend to introduce multi-responsive behavior that includes IS response<sup>[14b, 93]</sup>. For example, a programmed interpenetrating network hydrogel with poly(acrylic acid) and poly(N-isopropylacrylamide) was reported by Shang and coworkers<sup>[93]</sup>. Poly(acrylic acid) can respond both to pH and ionic strength due to the presence of the carboxylic acid group. Note that the actuating kinetics of IS responsive MAMs are in general slower than other response mechanisms like pH, temperature, or electric-triggered redox, taking 20–30 min to reach equilibrium<sup>[14b, 92]</sup>. This is likely due to the hindered transport rate of different ions within the hydrogel network. Theoretically, the response kinetics are also affected by the specific size, shape, and chemical components of the hydrogel. IS responsive MAMs with faster kinetics and better sensitivity are a promising direction for future studies in this area.

#### 4.4 Magnetic field-responsive MAMs

Magnetic field response is a simple and well understood method of remotely driving actuation<sup>[94]</sup>. Magnetic field responsive MAMs (MFRMAMs) are mostly composites of hydrogels mixed with magnetic nanoparticles (MNPs). Typically, MNPs are entrapped, either covalently or non-covalently, within the hydrogel network of the material. When a magnetic field is applied, MNPs are drawn along the direction of the field, pulling parts of the gel structure with them. MNPs encompass a wide variety of magnetic nanostructures, including single particles, linear arrays, or 2D structures. The application of magnetic fields during the synthesis of MFRMAMs can also direct the alignment of MNPs, programming the gel response by organizing the MNPs into isotropically or anisotropically aligned structures within the hydrogel matrix.

**4.4.1 MFRMAMs with randomly distributed MNPs**—MAMs with randomly distributed MNPs are among the most common MFRMAMs, as they do not require extra steps during synthesis to align the particles<sup>[95]</sup>. Without any specific arrangement of the MNPs, the actuation of these MAMs is simple, and the material moves toward the magnetic



field. In contrast, spatially organizing the MNP can generate more specific responses that have an inherent directionality. Such patterned MNP-doped materials are discussed in detail in the subsequent section 4.4.2. A good example of randomly organized MNP materials was developed by Haider and coworkers<sup>[95a]</sup> where they dispersed alginate coated Fe<sub>3</sub>O<sub>4</sub> nanoparticles in a polyacrylamide hydrogel (Figure 8a). The strength of the gel could be modulated through metal-cation crosslinking of the alginate components, here using Fe<sup>3+</sup> to obtain an ultimate tensile strength of up to ~1MPa. Though increasing the nanoparticle content gradually decreased the mechanical strength, the MFRMAMs had a larger response amplitude with the inclusion of more Fe<sub>3</sub>O<sub>4</sub> MNPs. The MFRMAMs would bend to the direction of magnetic field at any orientation, highlighting an advantage of this MFRMAM strategy. Similar work was conducted by Caykara et al<sup>[95b]</sup>, where MNPs were randomly distributed in a poly(N-tertbutylacrylamide-co-acrylamide) hydrogel matrix, creating a magnetically actuatable composite.

Though MFRMAMs can be directly actuated by magnetic force, a slightly more complex mechanism to create MFRMAMs is to incorporate MNPs with thermal responsive polymers, such as pNIPAM. By applying an alternating magnetic field (AMF), heat is produced by MNPs that triggers the thermal response of the hydrogel matrix<sup>[94b, 96]</sup>. Satarkar et al.<sup>[96a]</sup> fabricated such a Fe<sub>3</sub>O<sub>4</sub>/pNIPAM MFRMAMs composite. Upon application of AMF, the hydrogel collapsed and the microfluidic channel was toggled to the open state (Figure 8b). They further demonstrated the responsivity of this material could be tuned by MNP content and programmed geometry. In comparison with direct magnetic field actuation, the AMF-triggered, indirect thermal response of MFRMAMs tends to have larger actuation magnitudes.

**4.4.2 MAMs with organized MNPs**—Offering more precise movement control, MFRMAMs with organized MNPs represent an emerging area in magnetically responsive materials. MNPs can be pre-aligned prior to hydrogel formation by applying an external magnetic field, then polymerizing the MAM to freeze the MNP spatial arrangement into the gel network. Huang et al. <sup>[97]</sup> reported the fabrication of soft robot MAMs with programmable moieties, in which a “head” and “tail” region were separately programmed with different alignments of MNPs during the photopatterning of the bulk gel (Figure 8c). The authors found that the orientation of MNPs dictated the self-folding behavior of the different moieties, which determined the final morphology of the material. The MAM architecture (helical tail vs. flat tail) and magnetic field rotation were found to affect the movement velocity of the designed soft robot, creating a highly programmable MFRMAM design.

MAMs programmed by the alignment of MNPs demonstrate a practical way of fabricating functional soft robots with different geometries and propulsion styles. Compared to those with randomly aligned MNPs, MFRMAMs with organized MNPs show great promise in developing more sophisticated MAMs with programmable function.

## 4.5 Electrical field

Electrical field responsive MAMs (EFRMAMs) are usually responsive to one of two types of electrical stimuli either static or redox-based. For static electrical stimulation the physical deformation of the MAM directly results from the application of an electrical voltage<sup>[98]</sup>. In contrast, the redox-based EFRMAMs include a redox active group within the hydrogel that undergoes an electrochemical reaction by an applied electric field<sup>[25, 99]</sup>. Examples of such materials are given in Figure 9, and the unique mechanisms and advantages of each type of EFRMAM are described below.

**4.5.1 Static type**—Static type EFRMAMs are triggered by the formation of osmotic gradients when the material is exposed to static electric field. In these cases, polyelectrolytes in a material, such as salts, are electrostatically attracted to oppositely charged electrodes. This disrupts the chemical equilibrium within the material, and causes a difference in osmotic pressure throughout the material. Water is then drawn along the osmotic pressure gradient, resulting in anisotropic swelling of the EFRMAMs that causes material bending.

The bending behavior of static type EFRMAMs can be programmed through the types of polyelectrolytes in the system (i.e. polyanions or polycations). For example, an electrically actuated hydrogel walker was developed by Morales et al<sup>[100]</sup>. The two “legs” of this MAM were made of poly(acrylamide-co-sodium acrylate) and poly(acrylamide-co-quaternized dimethylaminoethyl methacrylate), respectively. Upon switching the electric field direction, the different legs switched between bending in a “pushing motion” and “pulling motion”, working like “legs” to propel the walker forward (Figure 9a). This chemical and geometric programming of the two legs allows the hydrogel walker to keep moving without relying on ratcheted surfaces or specific external conditions that other soft robotic walkers typically employ. The response of EFRMAMs can also be programmed by the presence of counterions to drive differential responses under certain conditions. Jiang et al.<sup>[101]</sup> studied the bidirectional bending behavior of EFRMAMs that were made of a copolymerized hydrogel of acrylic acid and N,N-dimethyl acrylamide. This copolymerization combines both polycation and polyanion together, and this resulted in a bidirectional bending behavior. This was found to be due to differential movement speeds of counterions such as H<sup>+</sup> in the system, and the kinetic difference in this counterion migration induced the bidirectional bending.

Recently, studies have begun focusing on making nanocomposite EFRMAMs with electrically conductive materials such as graphene<sup>[102]</sup> and carbon nanotubes<sup>[103]</sup>. Two main benefits of making nanocomposites with conductive materials have been identified in the literature. First, the inclusion of conductive materials increases the charge transport rate inside the EFRMAMs, leading to more rapid response kinetics. Additionally, nanocomposite EFRMAMs show better mechanical strength than EFRMAMs without these modifications, though this may hinder the actuation of hydrogel MAMs at higher concentrations<sup>[103b]</sup>. Thus, optimizing the content of conductive nanomaterials is important for EFRMAMs to obtain better electrical responding performance.

The static mechanism of EFRMAM response also has the advantage of giving remotely controlled actuation, similar to light responsive or MFRMAMs. However, the remote control

of EFRMAMs is less convenient than other remotely actuated MAMs, due to the specific requirement of salts in the solution.

**4.5.2 Redox type**—In contrast to the static type, redox-type EFRMAMs use an electrical current to drive a redox reaction within the hydrogel. This modulates the charge and the hydration state of the material, resulting in actuation. Importantly, this mechanism is distinct from the chemically-triggered redox responsive MAMs introduced in Section 4.3.2, as the electrons necessary for reduction are provided by electrical current, not chemical reactions. However, the response of redox-type EFRMAMs is most similar to that of the chemical redox MAMs.

For example, Xue et al.<sup>[25]</sup> reported a supramolecular peptide hydrogel that can be actuated by electrically-induced redox reactions. The hydrogel was modified with dihydroxyphenylalanine (dopa) as the redox active moiety that can be oxidized into dopaquinone through electrochemical reaction (Figure 9b). The oxidation of dopa greatly decrease hydrophilicity of the material, causing hydrogel deswelling that was easily reversed by reducing the dopaquinone back to dopa electrochemically. The actuation of these types of EFRMAMs does not necessarily rely on the polyelectrolyte composition of the medium, which can be an advantage in certain systems over static-type MAMs.

In both mechanisms of EFRMAM response, the electrochemical stability of the material under the applied voltage must be considered, which can limit some of the possible material components and applications. However, these considerations are necessary to avoid the production of undesired byproducts or permanent damage to the hydrogel, both of which could potentially compromise the reversibility of EFRMAMs.

## 4.6 Bioactuation

A novel example of programming MAM responsivity is the incorporation of biological components, such as cells or bacteria, to drive mechanical actuation (Figure 10). This is most often accomplished using muscle cells, with cardiac and skeletal tissues each having unique responsivity<sup>[104]</sup>. Both cell types work by creating an electrochemical potential, called an action potential, across the surface of the cell. This triggers an intracellular calcium release, which promotes binding of myosin motor proteins to actin fibers. Myosin then consumes ATP to pull on the resultant complex, resulting in mechanical force on the material that can be up to mN<sup>[105]</sup>.

The stimulus to which these MAMs respond is programmed by the cell type that is included. Actuators that require spontaneous contraction often employ cardiomyocytes, which generate their own action potentials and will continue to actuate in the presence of glucose as an energy source<sup>[106]</sup>. Cardiac-derived muscle cells are also responsive to electrostimulation, and many of these “bio-hybrid” MAMs utilize microelectrodes to achieve a more controlled force producing response. While spontaneous contraction of skeletal muscle can occur<sup>[104a]</sup>, it is not as regular and reliable as that of cardiac tissue. Therefore, skeletal muscle-based bioactuator materials tend to rely on electrostimulation to produce forces<sup>[107]</sup>. However, this provides more control and programmability of the response,

allowing for the actuator to be stopped and started as necessary, and to tune the frequency and magnitude of actuation.

Bioactuators offer unique advantages and challenges as compared to other MAMs. One notable limitation is the necessity to maintain the cellular component of these structures in a medium that provides glucose, salts, and other supplements, and preventing metabolic wastes from accumulating to toxic levels. These factors do, however, make bioactuated MAMs particularly well-suited for biomedical applications, such as those discussed in Section 5 below.

#### 4.7 Mechanical force-responsive MAMs

While the concept of a “mechanically active material” most notably includes materials that produce mechanical force in response to some stimulus, the ability to sense and respond to external forces is another type of mechanical activity. In order to be responsive to external mechanical forces, MAMs have been programmed with different signal outputs, including structural color<sup>[34, 108]</sup>, voltage production<sup>[109]</sup>, changes in electrical resistance<sup>[110]</sup>, and fluorescent signaling<sup>[24]</sup>.

Photonic crystal hydrogel MAMs (PCMAMs) are naturally responsive to mechanical force. The programmability of PCMAMs is determined by its crystal constant, a parameter related to the size and distance of periodic structures within the material. Tuning this crystal constant can allow for the production of structural color within the visible spectrum, making even small applied forces easy to identify. Any stretching, pressing, poking, or bending changes the distance between repeating units of the photonic crystal, therefore inducing this chromatic switching<sup>[34]</sup>, making PCMAMs a facile tool to identify externally applied forces.

Förster resonance energy transfer (FRET) is a fluorescence technique that has been broadly used to measure forces and distances in scientific studies<sup>[111]</sup>. Since the application of external force results in hydrogel deformation, this deformation may change the distance between two fluorophores embedded in the gel network<sup>[112]</sup>. This hypothesis was tested by Merindol et al.<sup>[24]</sup> by synthesizing a DNA-based hydrogel with FRET pairs that are non-covalently bound together. Stretching of the hydrogel separates the quencher and fluorophore and leads to a FRET-based fluorescence change that is used for imaging force density within the gel.

In addition to producing a light or color signal that can be easily observed by eye, MAMs that can output electrical signal have also been developed for integration into electronic devices. This electrical signaling includes producing voltage or changing resistance. These materials, known as triboelectric hydrogel MAMs, are of great interest for mechanical force sensing and energy conversion. In one example, He and colleagues generated a polyacrylamide/silk fibroin composite MAM that detected a wide range of strains and compressions and responded by changing its electrical resistance as well as output voltage signal<sup>[113]</sup>. Despite their sensitivity, these triboelectric MAMs can only indicate the magnitude of an applied force, and cannot provide spatial information regarding the force location. Nevertheless, triboelectric MAMs could represent an important mechanism in future applications, such as soft wearable devices.

## 4.8 Multi-responsive actuating systems

Recently, the concept of multi-responsive MAMs (M-MAMs), those with responsivity to several stimuli rather than just one, has been studied with increasing depth<sup>[114]</sup>. Generally, the broad responsivity of such MAMs is programmed by combining different responsive moieties together in one material system, which brings increased material complexity but also new applications for MAMs.

There are three major approaches in the existing body of literature toward designing M-MAMs. The first approach is copolymerization of different functional monomers or oligomers. For example, Sun et al<sup>[114a]</sup> synthesized poly(N-isopropyl acrylamide-co-acrylamide) and poly(2-(dimethylamino)ethyl methacrylate-co-2-acrylamido-2-methyl propane sulfonic acid) to create an M-MAM sensitive to temperature, pH, and salt concentration. The second approach is to combine hydrogels with different responsivity together physically, rather than chemically, in order to “add up” their responsivities in the resultant M-MAM. This method includes making hydrogels with multiple parts or layers of different hydrogels<sup>[114b, 114c]</sup>, or by building interpenetrating polymer networks of responsive polymers<sup>[114d]</sup>. The final approach is to synthesize hydrogels doped with various nanomaterials, such as graphene<sup>[114e, 114g, 114h]</sup>, Fe<sub>3</sub>O<sub>4</sub><sup>[114f]</sup>, carbon nanotubes<sup>[114j]</sup>, and others<sup>[114k]</sup>. These nanostructures can confer responsivities to the hydrogel matrix surrounding them, such as the carbon nanotube-containing MAM designed by Li et al. that responds to light, electricity, humidity, and volatile organic compounds<sup>[114j]</sup>. Importantly, these three approaches are not exclusive to each other, and these approaches are often combined to create M-MAMs.<sup>[114a, 114b, 114e]</sup>

The M-MAMs open a new gateway for high-level design of MAMs for more complex applications. While most of the “primary responsivities” have been well-studied, studying the integration of the multiple responses and enhancing precision in controlling them is a broad horizon in the future of programmable MAMs.

## 5. Applications of MAMs

MAMs encompass a wide variety of materials, sensitivities, and synthesis techniques that all work to program certain responses. Each unique combination of these factors creates a MAM with specific advantages and disadvantages that dictate how that material can be used. Here, we discuss the applications in which certain MAMs have been demonstrated in the scientific literature, and their implications for future work in the field.

### 5.1 MAMs Towards Soft Robotics

A traditional robot is defined as a machine that is capable of carrying out a complex series of actions automatically<sup>[115]</sup>. Soft robotics represents a nascent sub-field of traditional robotics where the robot is primarily comprised of a compliant or soft material that aims to emulate biological systems.<sup>[116]</sup> There is some controversy in the field as how to distinguish a soft matter actuator from a soft robot. For some researchers, a soft robot is indistinguishable from a soft actuator<sup>[117]</sup>, while for others soft actuators are a functional component of a soft robot<sup>[118]</sup>. In this review, we will adopt a more strict definition of a soft robot as a

sophisticated system that includes one or more soft actuators to generate a series of actions. Based on this definition, the vast majority of work self-described as “soft robotics” is more formally soft actuators. Regardless, we see these more complex MAM actuators as a step toward constructing soft robotic systems in the near future. In this section, we introduce hydrogel MAMs that may become components of soft robotic systems through three of the most common actuation approaches: magnetic, biological, and pressure-based actuation.

**5.1.1 Toward Magnetically Actuated Robotic Systems**—Magnetic actuation of robotic systems is well-suited for this application because it affords a convenient method for remote and untethered actuation of MAMs that has been favored in past studies. [114f, 116d, 116h] The magnetic actuation can be further classified as paramagnetic actuation and ferromagnetic actuation. For paramagnetic actuation, the hydrogel robots are exclusively attracted to the direction where magnetic field is greatest. This process does not distinguish the polarity of the magnetic field. For example, Tang et al.<sup>[116b]</sup> reported a “DNA robot” with magnetic field driven navigational locomotion (Figure 10a). The paramagnetic particles incorporated within this DNA hydrogel provide efficient actuation, while the DNA network provides elasticity and biocompatibility. The soft and deformable hydrogel robots were also demonstrated to move through confined spaces, showing potential applications for drug delivery.

For ferromagnetic actuation, the hydrogel robots are sensitive to the polarity of the magnetic field. This sensitivity increases the complexity of the robot’s actuation and enables diverse multimodal locomotion. For example, a “milli-robot” with a ferromagnetic head and thermo-responsive tail was reported by Du et al.<sup>[116c]</sup>. The head is made of a pNIPAM hydrogel with NdFeB microparticles which were magnetized by a strong external magnetic field. The resultant magnetization and magnetic coercivity of NdFeB particles ensure the ferromagnetic properties of the millimeter sized “robots”. Diverse multimodal locomotions, such as crawling, rolling, swinging, and helical propulsion, were observed and studied (Figure 10b).

**5.1.2 Toward Biologically Actuated Robotic Systems**—Bio-actuation is a fascinating yet challenging approach to fabricate hydrogel robotics. By incorporating mammalian cells or bacteria, hydrogel robots can be actuated by harnessing the power produced by these biological systems. This does, however, require that the hydrogel be biocompatible and have sufficient structural stability for the cells and bacteria to attach to. A self-swimming microbial “robot” has been created and reported by Higashi et al.<sup>[116e]</sup>. Flagellated bacteria were attached onto the tail of a hydrogel made of bacterial cellulose, and the flagellar beating provided the desired motility of the MAM. The self-swimming microbial robot demonstrated a moving speed of 4.8  $\mu\text{m/s}$ . However, one disadvantage of microbial robot is that the direction of locomotion is arbitrary, because it is difficult to direct the movement of bacteria. A more delicate bio-actuated hydrogel robot was developed by Morimoto et al.<sup>[116f]</sup> In their work, skeletal muscle cells were loaded onto Matrigel (a biologically derived hydrogel polymer), and the contraction of the cultured muscle tissue was controlled by applying electrical stimulation with gold electrodes (Figure 10c). In this way, the bio-actuated hydrogel “robots” was directly guided by the electrical signal input.

The “robot” also showed large actuation amplitudes ( $\sim 90^\circ$ ) and the biological components remained viable for over a week.

**5.1.3 Toward Pressure Actuated of Robotic Systems**—Pressure actuation refers to the locomotion of soft robotic materials caused by altering fluid pressure inside the MAMs. This kind of soft robot usually has an asymmetrical cavity inside that produces anisotropic force, which determines the direction of the actuation and locomotion. This strategy has already been widely adopted in non-hydrogel robotic systems<sup>[119]</sup>. However, its implementation in MAM-based hydrogel actuators is challenging, due to the mechanical softness of hydrogels that may deform or rupture under pressure changes. At least one group has addressed this concern though, as Zhang et al. strengthened alginate hydrogels by physically crosslinking polyacrylamide into the composite network<sup>[116g]</sup>. The hydrogel was programmed with this characteristic asymmetric cavity, which caused bending under hydraulic pressure (Figure 10d). This hydraulic pressure-driven hydrogel “robot” was demonstrated to grip a 7 grams cylindrical simulated cargo underwater.

## 5.2 MAM Valves in Microfluidics

An emerging application for MAMs in research and industry is in microfluidics. Microfluidic devices use micron-sized channels to control fluid flow rates and mixing, as well as sensing and separating different liquids based on fluid properties. In these devices, MAMs are applied as valves for flow control (Figure 11). In general, MAMs are particularly useful for this application due to their rapid response time (less than 1 second<sup>[120]</sup>), programable sensitivity to a variety of stimuli as described above, and their ease of incorporation into polymeric microfluidic devices, being hydrogel polymers themselves.

Hydrogel MAM-based microfluidic valves can be either remotely controlled, or self-controlled. On the spatial scale of microfluidics, traditional mechanical actuators can be difficult to implement. Therefore, remotely actuated valves are needed to manually control flow in these systems. Some groups have used photothermally activated hydrogels to create microfluidic valves which can be opened and closed with NIR light<sup>[120]</sup>. The concept of a photothermally triggered fluid control has been expanded recently to include not only valves, but microfluidic reservoirs of photothermally triggered material that pumps fluid into the system under photoactivation<sup>[121]</sup>. In this work, Fu and colleagues used a graphene oxide-pNIPAM system to control flow of fluid through their microfluidic device, and were able to modulate the pumping rate through changing the intensity and frequency of illumination with an 808 nm NIR light source. Light responsive MAMs do not only offer remote control of the system, but also a focused laser light provides a high level of spatiotemporal control over the valve actuation. Such control can also be achieved in electro-actuated valves in systems where microfluidics are integrated with microprinted circuitry<sup>[122]</sup>.

Another application is in creating a valve that responds to chemical stimuli, such as pH changes or biomolecule concentration, on rapid time scales<sup>[123]</sup>. In this way, the system is able to control its own behavior under the addition of chemical inputs. This self-control is a

unique advantage of MAMs in this application, and could be further developed in the future to aid in sensing toxins, biomarkers, or system imbalances in water quality testing, industrial quality control, or medical diagnostics.

### 5.3 Biomedical Applications of MAMs

Materials with programmable mechanical responses, such as MAMs, can be widely applicable in the biomedical sciences. From precise mechanical stimulation of cells to moving drugs toward their targets, MAMs have important applications in medicine as well as research and provides a unique niche for these mechanically active hydrogels. Many of the actuating mechanisms of these materials, such as thermal, IR, or magnetic stimulation, are compatible with *in vivo* and clinical work. The programmability of the material responses also makes them favorable for research applications, where specificity and spatiotemporal accuracy can enhance our understanding of biology at a molecular level. Here, we discuss some of the promising new work employing programmable MAMs in the biomedical sciences.

**5.3.1. MAMs Toward the Study of Cell Biology**—MAMs have been used for decades in biological research, with one of the earliest applications being the use of NIPAM-coated cell culture plates for temperature controlled, non-enzymatic cell release<sup>[124]</sup>. More recently developed applications leverage the benefits of specific polymeric actuators, such as biocompatibility, ease of modification, and spatiotemporal control of response, to study the roles of mechanical stimuli in cell biology. These technologies can be applied to multiple cell types and cellular processes. Advances in microfabrication have allowed for integration of actuators into “on-chip” devices, including a recent example of a thermoresponsive actuator capable of single-cell mechanical manipulation, placing programmable hydrogel actuators on the forefront of biological research techniques<sup>[125]</sup>.

Actuable MAMs are able to profoundly influence biology, particularly in cell types that are known to exist in mechanically active environments, such as cardiac, musculoskeletal, and orthopedic tissues. Magnetically responsive MAMs have been used to mechanically stimulate stem cells, directing their maturation toward the osteoblastic lineage<sup>[126]</sup>. Electrostimulation of a carbon nanotube-impregnated composite MAM has also been shown to direct skeletal muscle growth and differentiation.<sup>[127]</sup>

Light-responsive MAMs are particularly advantageous for cell studies, as they allow one to control mechanical inputs at higher spatiotemporal resolution than that afforded by bulk bioreactors, which are the current standard in the field. One example of this is the optomechanical actuator (OMA), a light-responsive MAM developed by Salaita et al. The OMAs, pNIPMAm-AuNR composites nanoparticles (Figure 12a) that collapse when exposed to 785 nm NIR light (Figure 12b), apply mechanical stimulation to cells through modification of their surface with cell adhesion ligands (Figure 12c). In these studies, mechanical stimulation with these MAMs enhanced differentiation and alignment of muscle progenitor cells<sup>[57]</sup> (Figure 12d), fibroblast actin polymerization (Figure 12e), and T cell calcium signaling (Figure 12e)<sup>[26]</sup>. In the study of muscle cells in particular, the spatial resolution afforded by light responsivity as opposed to other MAM mechanisms allowed



for study of differentiation mechanisms on a sub-cellular level. Using light also avoids confounding biological effects, as some chemical as well as electrostimulation have been known to influence muscle cell growth.

A final application of MAMs in cell biology is studying cancer mechanobiology. Solid tumor cells are known to be influenced by local mechanical conditions in the body. Researchers have quite recently begun to incorporate actuating materials with the ability to specifically program responses to study cancer biology in this way<sup>[128]</sup>. Lim et al. used a bilayer, thermoresponsive MAM to apply periodic compressive forces to tumor cell clusters, enhancing growth factor and angiogenic factor expression and providing novel insight into the role of force in tumorigenesis.

Using responsive hydrogel MAMs to study the role of mechanical forces in cell biology is still an emerging approach with these materials. However, as the focus in this field continues to turn toward providing the most biomimetic environment for cells *in vitro*, the incorporation of mechanical forces with programmable, actuating hydrogels will offer novel insight into development and disease.

**5.3.2. Tissue Engineering Applications of MAMs**—As in cell biology, the field of regenerative medicine is beginning to turn to programmable hydrogel actuators as biomaterials to promote tissue growth and healing. Natural tissues such as lung, muscle, and endothelial cells are subject to highly dynamic mechanical environments. However, current tissue engineering scaffolds are static and hence poorly reproduce this dynamic property of natural tissues. MAMs offer a solution by provide a material with tunable mechanical properties. While the use of MAMs *in vivo* is limited at this time, this field will likely expand as researchers seek mechanisms to apply MAMs toward solving clinical challenges. These applications leverage the biocompatibility of gels and polymers with their tunable mechanical and chemical properties to promote tissue formation through therapeutic force application. A current example of MAMs used for tissue regeneration is the biphasic ferrogel, an alginate-based hydrogel material impregnated with iron oxide nanoparticles. Under an oscillating magnetic field, implanted gels applied cyclic mechanical loading to the tibialis anterior, and were able to enhance healing in a mouse muscle injury model<sup>[129]</sup>. As the tissue engineering field continues to grow, MAMs offer an opportunity to incorporate the dynamics of the physiological environment for enhanced biomimicry.

In another study, 4D printing was used to create hydrogel structures containing mouse stromal cells that would change shape from a sheet to a tube conformation in cell media. While creating microtube structures challenges the spatial resolution of current printing technologies, the rolled geometry resulting from printing a MAM created capillary-like structures with internal diameters as small as tens of microns, opening the door to incorporate vascularization in future tissue engineered constructs<sup>[130]</sup>.

**5.3.3. MAMs as Drug Delivery Vehicles**—Another notable application of MAMs in the biomedical sciences is drug delivery. It is important to distinguish between non-mechanically mediated drug release mechanisms and mechanically mediated drug delivery platforms, even though sometimes, this distinction is subtle. For example, protease-

mediated degradation that releases a drug bound to a hydrogel matrix is not necessarily mechanical<sup>[131]</sup>. However, if an enzymatic activity changes the hydrophilicity or crosslinking density in a polymer, leading to hydrogel swelling that allows for release of an entrapped drug<sup>[132]</sup>, then this includes a mechanical component. Other examples of mechanically driven drug delivery include MAMs that physically “grip” the drug, and can be triggered to release it at a certain site. Here, we highlight several examples of MAMs in drug delivery that satisfy this distinction from classical delivery mechanisms.

The high degree of programmability and specificity of response conditions makes MAMs optimal for carrying drug molecules to specific sites in the body and releasing these drugs under either native or remotely triggered conditions. Remote triggering of drug localization and release is highly desirable in medical applications, providing high specificity of delivery without invasive procedures. Many remotely actuable hydrogels are compatible with biomedical applications, such as magnetic. Cezar et al. applied the biphasic ferrogel, a hydrogel MFRMAM containing a gradient of iron oxide for programmed magnetic responsiveness, for controlled release of the chemotherapeutic drug mitoxantrone, as well as release of cells for therapeutic purposes<sup>[133]</sup>. Other groups have employed NIR-driven molecule release as a remotely actuated delivery mechanism, using light to physically deform the MAM delivery system and release chemotherapeutic agents at a targeted site [106c, 134].

While remote actuation through light or magnetic field manipulation is viable in some scenarios, another desirable mechanism for drug release is through sensing and self-actuation of the material without external intervention. This allows the drug to be released when and where a programmed stimulus is present, even deep inside the body where external stimulation methods would be ineffective. Indeed, prevalent areas of research for these materials are in the gastrointestinal system, where dramatic changes in pH at various stages provide a stimulus to swell hydrogels and trigger drug release<sup>[135]</sup>. Similarly, such materials can protect protein therapeutics, such as insulin or antibody treatments, from the denaturing environment of the stomach, providing a potential to increase efficacy and remove the need for injections of such drugs<sup>[136]</sup>. Chemical responsiveness can also be used to monitor and treat conditions. Li et al. developed a multi-responsive MAM containing the enzymes glucose oxidase and catalase, and an insulin drug payload as a potential diabetes therapeutic. In the presence of glucose, the enzymes create a local pH change that unfolds the protein hydrogel, releasing insulin<sup>[137]</sup>.

By providing the ability to specify the location and conditions of drug release, the unique properties MAMs can remove off-target side effects and increase drug efficacy by ensuring delivery to the appropriate tissue. One example that combines the controlled release of programmable hydrogel MAMs with their ability for active transport is a recent design of a bio-hybrid robot for chemotherapeutic delivery. A bio-actuated cardiomyocyte-laden hydrogel structure was designed to move through a fluid medium, powered by the spontaneous contraction of the embedded cells. At specific laser illumination sites, the construct released its drug payload through photothermal actuation, allowing it to target specific cells in a monolayer<sup>[106c]</sup>. These examples indicate a strong future for MAMs in drug delivery, where

their programmable specificity is a desirable characteristic to remove off-target side effects of drugs while ensuring efficient delivery to targeted cells.

#### 5.4 MAMs as Smart Skin Materials

Mechanically active smart skins refer to hydrogel materials that can sense or produce mechanical forces. Like other MAMs, these materials can respond to a wide variety of inputs, but are unique in their applications and design. In general, smart skin MAMs are thin, mechanically robust, compliant, and sometimes biocompatible. For example, we reported a strain-accommodating smart skin that can change its color in response to thermal heating, mechanical stretching, as well as illumination including ambient sunlight (Figure 13a)<sup>[34]</sup>. Similar to the skin structure of the chameleon, the force generated by responsive domains in the MAM changed the lattice space of photonic crystals. Compare to conventional chromatic responsive smart skins, which often results large volume change, our design applies a secondary strain-accommodating matrix to accommodate the photonic crystal (PC) domains. According to both computational and experimental results, the strain-accommodating matrix absorbs the strains produced by the PC domains, allowing the bulk material to remain a constant size. This multi-responsive, strain-accommodating smart skin MAM is very promising for applications such as camouflage, sensing, and anti-counterfeiting.

Another example of a MAM smart skin is the triboelectric, energy-harvesting skin reported by Liu et al.<sup>[109]</sup>, in which the smart skin is considered as a convenient mechanoresponsive electric generator (Figure 13b). When applied to the skin, the hydrogel MAM senses bending or stretching, and converts this mechanical energy to electricity through the deformation of dielectric polymers. This concept of harvesting the energy of everyday motion into electricity is a novel application for which MAM smart skins are uniquely suited. It is likely even more work will be conducted in this area, integrating the fundamental synthesis of smart skins with top-down design parameters to further explore the practical applications of these MAMs.

#### 5.5 MAMs as Tools for Force Spectroscopy

Another emerging application for force-generating MAMs is in the area of biophysical chemistry and mechanobiology. To study the response of individual proteins and polymer chains to the application of external forces, one typically employs single molecule force spectroscopy tools. These methods include atomic force microscopy, optical tweezers, and magnetic tweezers. Indeed, single-molecule force spectroscopy has revealed hidden domains (cryptic domains) within mechano-sensing proteins<sup>[138]</sup> and have measured the growth kinetics of single metathesis polymer chains<sup>[139]</sup>. One challenge with single molecule force spectroscopy methods is that these methods require a dedicated instrument that can only manipulate a single molecule at a time.

In principle, MAMs that are precisely controlled in space and time offer the potential to complement single-molecule methods, manipulating the forces applied to many molecules in parallel. This parallelized control of molecular mechanics allows one to study the dynamics of molecular unfolding, while also providing enhanced throughput compared to traditional

mechanical methods on the molecular scale (e.g. atomic force microscopy)<sup>[140]</sup>. MAMs can further enhance single molecule force spectroscopy, such as the DNA-based, force sensitive hydrogel designed by Merindol and colleagues<sup>[24]</sup>. These MAMs incorporate fluorescent reporters which sense and report stresses in 2D and 3D, providing additional spatial information compared to other force microscopy techniques.

Recently, our group has employed the polymer force clamp (PFC) (Figure 14) to study the mechanically unfolding of nucleic acid molecules<sup>[140]</sup>. PFCs are photo-responsive, micron-scale MAMs designed with a gold nanorod core and pNIPAM as its shell. Upon NIR laser irradiation, the heat produced by plasmonic effect of gold nanorod triggers the shrinkage of heat-sensitive polymer shell. The resulting piconewton-scale forces capable of opening fluorescently labeled DNA hairpin structures. The deformed hairpin then emits a signal can be observed by traditional fluorescence microscopy, making single molecule-level force spectroscopy more accessible.

## 6. Outlooks and Perspectives

In conclusion, programmable hydrogel-based MAMs have drawn great attentions not only for their responsivity but also their prospective applications. The component of these materials could be either derived from synthetic polymer or bio-macromolecules. In order to program MAMs with mechanical force related behaviors, either bottom-up or top-down approach has been reported in existing works and there are works adopting the two approaches at the same time. Generally, hydrogel-based MAMs respond to a variety of stimuli such as pH, temperature, biomolecules, magnetic field, electric field, etc. There is a growing trend to fabricate multi-responsive MAMs so that the response can be tailored more precisely. Finally, hydrogel-based MAMs have been reported with prospective applications such as soft robots, microfluidics, biomedical engineering, smart skins, and molecular force generator. The development of MAMs in future would combine with more sophisticated responsivity and more specific applications.

What does the future hold for MAMs? Anticipating how the field will evolve over the next few years is not easy, as there has been a rapid rate of new developments in MAMs. An important area for this field is honing the fabrication technologies used to create MAMs. The vast majority of current MAMs take the form of thin films, rods, and other simple shapes. While complex architectures have been achieved by assembling these rudimentary shapes together or creating rationally designed self-assembly structures, it is likely that improved 3D printers and lithography techniques over the next few years will allow the manufacture of exciting new MAM geometries.

As scientists begin to create MAMs more efficiently and with more varied architecture, the practical application of these materials is expected to grow as well. One area of expansion will be to create more advanced robotic systems, increasing the complexity of their functions and operations, along with programming more autonomy into these structures. Such self-actuating soft robots could fill a unique niche in both size and sensitivity that traditional robotics may not be optimized for.

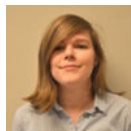
Medicine is another area with great potential for future MAM development. As drug delivery vehicles, MAMs have already shown great promise for specific localization and release of therapeutics. This could be particularly advantageous for cancer treatment, carrying toxic chemotherapy drugs directly to tumors and minimizing off-target effects. The sensing abilities of MAMs may also be further enhanced to develop a self-releasing insulin delivery platform, which may improve quality of life for diabetic patients. Additionally, MAMs will likely be further developed for regenerative medicine applications. Many bio-material strategies work to mimic the physiological environment of a target tissue in structure and chemical composition, and incorporating native mechanical cues is a logical next step in the field.

The role model for mechanically active hydrogels are often biological systems such as skins, muscles, cellular matrices, etc. Many studies are inspired from natural examples, such as smart skin systems that will likely see increased growth in the coming years, as their multi-responsive nature lends them to many applications across multiple industries. Photonic smart skin MAMs have great potential, ranging from microscale force sensing to next-generation camouflage and cloaking technologies. Biocompatible smart skins may also see development for medical sensing and diagnostics as at-home and point-of-care testing continues to gain popularity.

## Acknowledgement

This work is supported by NSF (1905947) and the NIH (R01 HL142866, R01 GM131099, and R01 GM124472).

## Biography



**Allison N. Ramey-Ward** received her B.S. degree in biomedical engineering from Virginia Commonwealth University in 2016. She is currently a Ph.D. candidate in the laboratory of Khalid Salaita at Emory University. Her research background involves musculoskeletal tissue engineering, and her current work involves developing novel biomaterials to investigate the role of cell-substrate mechanics in muscle cell growth and maturation.



**Khalid Salaita** is a Professor of Chemistry at Emory University. He obtained his Ph.D. with Prof. Chad Mirkin at Northwestern University (Evanston, IL) in 2006. From 2006–2009, Khalid was a postdoctoral scholar with Prof. Jay T. Groves at the University of California at Berkeley (USA). His group has pioneered the development of molecular force sensor,

hydrogel actuators, DNA mechanotechnology, and smart therapeutics. He is currently a member of the Enabling Bioanalytical and Imaging Technologies (EBIT) study Section and an Associate Editor of Smart Materials.



**Yixiao Dong** received her B.S. and M.S degree from Wuhan University of Technology. He is currently a Ph.D. candidate in Dr. Salaita research group at Emory University. His research background involves responsive hydrogels, functional nanomaterials, and smart polymer materials. His current work involves developing novel biomimetic nanocomposite hydrogel materials.

## References

- [1]. Patil H, Vaijapurkar S, J. Bionic. Eng 2007, 4, 19.
- [2]. Trimmer BA, Lin H.-t., Oxford University Press, 2014.
- [3]. Forterre Y, Skotheim JM, Dumais J, Mahadevan L, Nature 2005, 433, 421. [PubMed: 15674293]
- [4]. a) Zheng SY, Shen Y, Zhu F, Yin J, Qian J, Fu J, Wu ZL, Zheng Q, Adv. Funct. Mater 2018, 28, 1803366;b) Guo W, Li M, Zhou J, Smart Materials and Structures 2013, 22, 115028;c) Peng X, Liu T, Zhang Q, Shang C, Bai QW, Wang H, Adv. Funct. Mater 2017, 27, 1701962.
- [5]. Duraj-Thatte AM, Courchesne NMD, Praveschotinunt P, Rutledge J, Lee Y, Karp JM, Joshi NS, Adv. Mater 2019, 31, 1901826.
- [6]. Jani JM, Leary M, Subic A, Gibson MA, Mater Design 2014, 56, 1078.
- [7]. Chan HL-W, Li K, Choy CL, in Wearable Electronics and Photonics, (Ed: Tao X), Woodhead Publishing, 2005, 41;b) Zhang H, Zhou J, Shen J, Wang T, Xie D, Chen W, Appl. Phys. Lett 2018, 113, 152902.
- [8]. Teotia AK, Sami H, Kumar A, in Switchable and Responsive Surfaces and Materials for Biomedical Applications, (Ed: Zhang Z), Woodhead Publishing, Oxford 2015, 3.
- [9]. Ahmed EM, Journal of Advanced Research 2015, 6, 105. [PubMed: 25750745]
- [10]. Soutif J-C, Brosse J-C, Reactive Polymers 1990, 12, 3.
- [11]. a) Duracher D, Elaïssari A, Pichot C, Colloid and Polymer Science 1999, 277, 905;b) Heskins M, Guillet JE, Journal of Macromolecular Science: Part A - Chemistry 1968, 2, 1441;c) Zhao J, Su H, Vansuch GE, Liu Z, Salaita K, Dyer RB, ACS Nano 2019, 13, 515. [PubMed: 30574782]
- [12]. Lv C, Xia H, Shi Q, Wang G, Wang YS, Chen QD, Zhang YL, Liu LQ, Sun HB, Advanced Materials Interfaces 2017, 4, 1601002.
- [13]. a) Moe ST, Skjaak-Braek G, Elgsaeter A, Smidsroed O, Macromolecules 1993, 26, 3589;b) Gatej I, Popa M, Rinaudo M, Biomacromolecules 2005, 6, 61; [PubMed: 15638505] c) Qu X, Wirsén A, Albertsson AC, J. Appl. Polym. Sci 1999, 74, 3186.
- [14]. a) Lu B, Luo D, Zhao A, Wang H, Zhao Y, Maitz MF, Yang P, Huang N, Progress in Organic Coatings 2019, 135, 240;b) Zhou S, Wu B, Zhou Q, Jian Y, Le X, Lu H, Zhang D, Zhang J, Zhang Z, Chen T, Macromol. Rapid Commun 2020, 41, 1900543.
- [15]. Rothmund PWK, Nature 2006, 440, 297. [PubMed: 16541064]
- [16]. Tan ZJ, Chen SJ, Biophysical journal 2006, 90, 1175. [PubMed: 16299077]
- [17]. Le X, Lu W, Zhang J, Chen T, Advanced Science 2019, 6, 1801584.
- [18]. a) Sardesai AN, Segel XM, Baumholtz MN, Chen Y, Sun R, Schork BW, Buonocore R, Wagner KO, Golecki HM, MRS Advances 2018, 3, 3003;b) Liu X, Liu J, Lin S, Zhao X, Materials Today 2020.

- [19]. Abe K, Kawamata I, Shin-ichiro MN, Murata S, *Molecular Systems Design & Engineering* 2019, 4, 639.
- [20]. Khoury LR, Popa I, *Nat. Commun* 2019, 10, 1. [PubMed: 30602773]
- [21]. Wang L, Zhu L, Hickner M, Bai B, *Chem. Mater* 2017, 29, 9981.
- [22]. Cheng Y, Luo X, Payne GF, Rubloff GW, *J. Mater. Chem* 2012, 22, 7659.
- [23]. Cangialosi A, Yoon C, Liu J, Huang Q, Guo J, Nguyen TD, Gracias DH, Schulman R, *Science* 2017, 357, 1126. [PubMed: 28912239]
- [24]. Merindol R, Delechiave G, Heinen L, Catalani LH, Walther A, *Nat. Commun* 2019, 10, 1. [PubMed: 30602773]
- [25]. Xue B, Qin M, Wang T, Wu J, Luo D, Jiang Q, Li Y, Cao Y, Wang W, *Adv. Funct. Mater* 2016, 26, 9053.
- [26]. Liu Z, Liu Y, Chang Y, Seyf HR, Henry A, Mattheyses AL, Yehl K, Zhang Y, Huang Z, Salaita K, *Nat. Meth* 2016, 13, 143.
- [27]. Zhou Y, Duque CM, Santangelo CD, Hayward RC, *Adv. Funct. Mater* 2019, 29, 1905273.
- [28]. Dong Y, Wang J, Guo X, Yang S, Ozen MO, Chen P, Liu X, Du W, Xiao F, Demirci U, *Nat. Commun* 2019, 10, 1. [PubMed: 30602773]
- [29]. a) Ye C, Nikolov SV, Calabrese R, Dindar A, Alexeev A, Kippelen B, Kaplan DL, Tsukruk VV, *Angew. Chem* 2015, 127, 8610; b) Ye C, Nikolov SV, Geryak RD, Calabrese R, Ankner JF, Alexeev A, Kaplan DL, Tsukruk VV, *ACS Appl. Mater. Interfaces* 2016, 8, 17694.
- [30]. Lv C, Sun X-C, Xia H, Yu Y-H, Wang G, Cao X-W, Li S-X, Wang Y-S, Chen Q-D, Yu Y-D, *Sensors and Actuators B: Chemical* 2018, 259, 736.
- [31]. Zhao J, Liu P, Liu Y, *Langmuir* 2018, 34, 7479. [PubMed: 29860837]
- [32]. a) Zhao Z, Wang C, Yan H, Liu Y, *Adv. Funct. Mater* 2019, 29, 1905911; b) Takahashi R, Wu ZL, Arifuzzaman M, Nonoyama T, Nakajima T, Kurokawa T, Gong JP, *Nat. Commun* 2014, 5, 4490. [PubMed: 25105259]
- [33]. a) Zhang X, Pint CL, Lee MH, Schubert BE, Jamshidi A, Takei K, Ko H, Gillies A, Bardhan R, Urban JJ, Wu M, Fearing R, Javey A, *Nano Lett.* 2011, 11, 3239; [PubMed: 21736337] b) Ma C, Lu W, Yang X, He J, Le X, Wang L, Zhang J, Serpe MJ, Huang Y, Chen T, *Adv. Funct. Mater* 2018, 28, 1704568; c) Stoychev G, Guiducci L, Turcaud S, Dunlop JW, Ionov L, *Adv. Funct. Mater* 2016, 26, 7733; d) Lee BP, Konst S, *Adv. Mater* 2014, 26, 3415; [PubMed: 24596273] e) Wang X, Huang H, Liu H, Rehfeldt F, Wang X, Zhang K, *Macromol. Chem. Phys* 2019, 220, 1800562.
- [34]. [Dong Y, Bazrafshan A, Pokutta A, Sulejmani F, Sun W, Combs JD, Clarke KC, Salaita K, *ACS Nano* 2019, 13, 9918. [PubMed: 31507164]
- [35]. Pimpin A, Srituravanich W, *Engineering Journal* 2012, 16, 37.
- [36]. Shim TS, Kim SH, Heo CJ, Jeon HC, Yang SM, *Angew. Chem. Int. Ed* 2012, 51, 1420.
- [37]. Martella D, Nocentini S, Nuzhdin D, Parmeggiani C, Wiersma DS, *Adv. Mater* 2017, 29, 1704047.
- [38]. Wang X, Jiang M, Zhou Z, Gou J, Hui D, *Composites Part B: Engineering* 2017, 110, 442.
- [39]. Khoo ZX, Teoh JEM, Liu Y, Chua CK, Yang S, An J, Leong KF, Yeong WY, *Virtual and Physical Prototyping* 2015, 10, 103.
- [40]. Dong Y, Wang S, Ke Y, Ding L, Zeng X, Magdassi S, Long Y, *Advanced Materials Technologies* 2020, 5, 2000034.
- [41]. Odent J, Vanderstappen S, Toncheva A, Pichon E, Wallin TJ, Wang K, Shepherd RF, Dubois P, Raquez J-M, *Journal of Materials Chemistry A* 2019, 7, 15395.
- [42]. Li D, Xia Y, *Adv. Mater* 2004, 16, 1151.
- [43]. a) Manoukian OS, Matta R, Letendre J, Collins P, Mazzocca AD, Kumbar SG, in *Biomedical Nanotechnology*, Springer, 2017, 261; b) Khorshidi S, Solouk A, Mirzadeh H, Mazinani S, Lagaron JM, Sharifi S, Ramakrishna S, *Tissue Eng J. Regen. Med* 2016, 10, 715.
- [44]. Liu L, Jiang S, Sun Y, Agarwal S, *Adv. Funct. Mater* 2016, 26, 1021.
- [45]. Rabin B, Shiota I, *MRS bulletin* 1995, 20, 14.
- [46]. Luo R, Wu J, Dinh ND, Chen CH, *Adv. Funct. Mater* 2015, 25, 7272.

- [47]. Yao C, Liu Z, Yang C, Wang W, Ju XJ, Xie R, Chu LY, *Adv. Funct. Mater* 2015, 25, 2980.
- [48]. Liu J, Xu W, Kuang Z, Dong P, Yao Y, Wu H, Liu A, Ye F, *J. Mater. Chem. C* 2020.
- [49]. Wang J, Wang J, Chen Z, Fang S, Zhu Y, Baughman RH, Jiang L, *Chem. Mater* 2017, 29, 9793.
- [50]. Liu Y, Zhang K, Ma J, Vancso GJ, *ACS Appl. Mater. Interfaces* 2017, 9, 901. [PubMed: 28026935]
- [51]. Kularatne RS, Kim H, Ammanamanchi M, Hayenga HN, Ware TH, *Chem. Mater* 2016, 28, 8489.
- [52]. a) Augé A, Zhao Y, *RSC Adv.* 2016, 6, 70616;b) Ding Y, yan Y, Peng Q, Wang B, Xing Y, Hua Z, Wang Z, *ACS Applied Polymer Materials* 2020.
- [53]. Hua L, Xie M, Jian Y, Wu B, Chen C, Zhao C, *ACS Appl. Mater. Interfaces* 2019, 11, 43641. [PubMed: 31663325]
- [54]. Gorelikov I, Field LM, Kumacheva E, *Journal of the American Chemical Society* 2004, 126, 15938. [PubMed: 15584708]
- [55]. Payne EK, Shuford KL, Park S, Schatz GC, Mirkin CA, *The Journal of Physical Chemistry B* 2006, 110, 2150. [PubMed: 16471797]
- [56]. Mackey MA, Ali MRK, Austin LA, Near RD, El-Sayed MA, *The Journal of Physical Chemistry B* 2014, 118, 1319. [PubMed: 24433049]
- [57]. Ramey-Ward AN, Su H, Salaita K, *ACS Applied Materials & Interfaces* 2020.
- [58]. a) Acik M, Lee G, Mattevi C, Chhowalla M, Cho K, Chabal YJ, *Nature Materials* 2010, 9, 840; [PubMed: 20852618] b) Mak KF, Ju L, Wang F, Heinz TF, *Solid State Communications* 2012, 152, 1341.
- [59]. Shi K, Liu Z, Wei Y-Y, Wang W, Ju X-J, Xie R, Chu L-Y, *ACS Applied Materials & Interfaces* 2015, 7, 27289.
- [60]. a) Yang Y, Tan Y, Wang X, An W, Xu S, Liao W, Wang Y, *ACS Applied Materials & Interfaces* 2018, 10, 7688; [PubMed: 29363307] b) Cong H-P, Wang P, Yu S-H, *Chemistry of Materials* 2013, 25, 3357;c) Sun S, Wu P, *Journal of Materials Chemistry* 2011, 21, 4095.
- [61]. a) Lu L, Chen W, *Nanoscale* 2011, 3, 2412; [PubMed: 21523297] b) Shin S, Shin C, Memic A, Shadmehr S, Miscuglio M, Jung HY, Jung S, Bae H, Khademhosseini A, Tang X, Dokmeci M, *advanced functional materials* 2015, 25, 4486. [PubMed: 27134620]
- [62]. Zong L, Li X, Han X, Lv L, Li M, You J, Wu X, Li C, *ACS Applied Materials & Interfaces* 2017, 9, 32280.
- [63]. a) Kamenjicki M, Lednev IK, Asher SA, *The Journal of Physical Chemistry B* 2004, 108, 12637;b) Takashima Y, Hatanaka S, Otsubo M, Nakahata M, Kakuta T, Hashidzume A, Yamaguchi H, Harada A, *Nature Communications* 2012, 3, 1270.
- [64]. Ikejiri S, Takashima Y, Osaki M, Yamaguchi H, Harada A, *Journal of the American Chemical Society* 2018, 140, 17308.
- [65]. Zhao YS, Xuan C, Qian XS, Alsaied Y, Hua MT, Jin LH, He XM, *Sci Robot* 2019, 4.
- [66]. Ma C, Lu W, Yang X, He J, Le X, Wang L, Zhang J, Serpe MJ, Huang Y, Chen T, *Adv. Funct. Mater* 2018, 28, 1704568.
- [67]. Sun Z, Yamauchi Y, Araoka F, Kim YS, Bergueiro J, Ishida Y, Ebina Y, Sasaki T, Hikima T, Aida T, *Angewandte Chemie (International ed. in English)* 2018, 57, 15772.
- [68]. Zhao J, Su H, Vansuch GE, Liu Z, Salaita K, Dyer RB, *ACS Nano* 2018, 13, 515. [PubMed: 30574782]
- [69]. a) Chen F, Guo J, Xu D, Yan F, *Polymer Chemistry* 2016, 7, 1330;b) Zarzar LD, Kim P, Aizenberg J, *Adv. Mater* 2011, 23, 1442; [PubMed: 21433110] c) Nakagawa H, Hara Y, Maeda S, Hasimoto S, *Polymers* 2011, 3, 405;d) Han Z, Wang P, Mao G, Yin T, Zhong D, Yiming B, Hu X, Jia Z, Nian G, Qu S, Yang W, *ACS Appl. Mater. Interfaces* 2020, 12, 12010;e) Dai L, Ma M, Xu J, Si C, Wang X, Liu Z, Ni Y, *Chem. Mater* 2020, 32, 4324.
- [70]. Duan J, Liang X, Zhu K, Guo J, Zhang L, *Soft Matter* 2017, 13, 345. [PubMed: 27901170]
- [71]. a) Zhang K, Liang Y, Liu D, Liu H, *Sensors and Actuators B: Chemical* 2012, 173, 367;b) Topham PD, Howse JR, Fernyhough CM, Ryan AJ, *Soft Matter* 2007, 3, 1506. [PubMed: 32900105]
- [72]. a) Wang L, Topham PD, Mykhaylyk OO, Howse JR, Bras W, Jones RAL, Ryan AJ, *Adv. Mater* 2007, 19, 3544;b) Techawanitchai P, Ebara M, Idota N, Asoh T-A, Kikuchi A, Aoyagi T, *Soft*



Matter 2012, 8, 2844;c) Le X, Lu W, Xiao H, Wang L, Ma C, Zhang J, Huang Y, Chen T, ACS Appl. Mater. Interfaces 2017, 9, 9038. [PubMed: 28221748]

- [73]. Gibson KJ, Prominski A, Lee MS, Cronin TM, Parker J, Weizmann Y, Cell Reports Physical Science 2020, 1, 100080.
- [74]. Idili A, Vallée-Bélisle A, Ricci F, J. Am. Chem. Soc 2014, 136, 5836. [PubMed: 24716858]
- [75]. a) Cheng E, Xing Y, Chen P, Yang Y, Sun Y, Zhou D, Xu L, Fan Q, Liu D, Angew. Chem. Int. Ed 2009, 48, 7660;b) Guo W, Lu CH, Orbach R, Wang F, Qi XJ, Ceconello A, Seliktar D, Willner I, Adv. Mater 2015, 27, 73. [PubMed: 25377247]
- [76]. a)Greene AF, Danielson MK, Delawder AO, Liles KP, Li X, Natraj A, Wellen A, Barnes JC, Chem. Mater 2017, 29, 9498;b) Murase Y, Takeshima R, Yoshida R, Macromol. Biosci 2011, 11, 1713; [PubMed: 21919207] c) Nakahata M, Takashima Y, Hashidzume A, Harada A, Angew. Chem. Int. Ed 2013, 52, 5731;d) Wang B, Tahara H, Sagara T, ACS Appl. Mater. Interfaces 2018, 10, 36415;e) Liu X, Zhao L, Liu F, Astruc D, Gu H, Coord. Chem. Rev 2020, 419, 213406;f) Aramoto H, Osaki M, Konishi S, Ueda C, Kobayashi Y, Takashima Y, Harada A, Yamaguchi H, Chem. Sci 2020, 11, 4322. [PubMed: 34122890]
- [77]. Yoshida R, Ueki T, NPG Asia Materials 2014, 6, e107.
- [78]. Murase Y, Maeda S, Hashimoto S, Yoshida R, Langmuir 2009, 25, 483. [PubMed: 19063637]
- [79]. Tabata O, Kojima H, Kasatani T, Isono Y, Yoshida R, “Chemo-mechanical actuator using self-oscillating gel for artificial cilia”, presented at The Sixteenth Annual International Conference on Micro Electro Mechanical Systems, 2003. MEMS-03 Kyoto. IEEE, 2003.
- [80]. Maeda S, Hara Y, Sakai T, Yoshida R, Hashimoto S, Adv. Mater 2007, 19, 3480.
- [81]. Li Z, Davidson-Rozenfeld G, Vázquez-González M, Fadeev M, Zhang J, Tian H, Willner I, J. Am. Chem. Soc 2018, 140, 17691.
- [82]. a) Culver HR, Clegg JR, Peppas NA, Acc. Chem. Res 2017, 50, 170; [PubMed: 28170227] b) Li F, Lyu D, Liu S, Guo W, Adv. Mater 2020, 32, 1806538.
- [83]. a) Sim HJ, Jang Y, Kim H, Choi JG, Park JW, Lee DY, Kim SJ, ACS Appl. Mater. Interfaces 2020, 12, 20228;b) Tong R, Yu H, Wang L, ChemistrySelect 2020, 5, 8858;c) Lee J, Ko S, Kwon CH, Lima MD, Baughman RH, Kim SJ, Small 2016, 12, 2085. [PubMed: 26929006]
- [84]. a) McDonald TO, Qu H, Saunders BR, Ulijn RV, Soft Matter 2009, 5, 1728;b) Hu J, Zhang G, Liu S, Chem. Soc. Rev 2012, 41, 5933; [PubMed: 22695880] c) Athas JC, Nguyen CP, Zarket BC, Gargava A, Nie Z, Raghavan SR, ACS Appl. Mater. Interfaces 2016, 8, 19066.
- [85]. Fern J, Schulman R, Nat. Commun 2018, 9, 1. [PubMed: 29317637]
- [86]. Zhang J-T, Cai Z, Kwak DH, Liu X, Asher SA, Anal. Chem 2014, 86, 9036. [PubMed: 25162117]
- [87]. a) Chen C, Dong Z-Q, Shen J-H, Chen H-W, Zhu Y-H, Zhu Z-G, ACS Omega 2018, 3, 3211; [PubMed: 31458578] b) Tang W, Chen C, Polymers 2020, 12, 625.
- [88]. a) Shin B, Ha J, Lee M, Park K, Park GH, Choi TH, Cho K-J, Kim H-Y, Science Robotics 2018, 3;b) Sun X-C, Xia H, Xu X-L, Lv C, Zhao Y, Sensors and Actuators B: Chemical 2020, 128620.
- [89]. Yin Q, Tu S, Chen M, Wu L, ACS Applied Polymer Materials 2020.
- [90]. Chang Q, Darabi MA, Liu Y, He Y, Zhong W, Mequanin K, Li B, Lu F, Xing MM, Journal of Materials Chemistry A 2019, 7, 24626.
- [91]. Chen X, Goodnight D, Gao Z, Cavusoglu AH, Sabharwal N, DeLay M, Driks A, Sahin O, Nat. Commun 2015, 6, 7346. [PubMed: 26079632]
- [92]. Wang Y, Huang W, Wang Y, Mu X, Ling S, Yu H, Chen W, Guo C, Watson MC, Yu Y, Proceedings of the National Academy of Sciences 2020.
- [93]. Shang J, Theato P, Soft Matter 2018, 14, 8401. [PubMed: 30311935]
- [94]. a) Shi W, Huang J, Fang R, Liu M, ACS Appl. Mater. Interfaces 2020, 12, 5177; [PubMed: 31916743] b) Han IK, Chung T, Han J, Kim YS, Nano Convergence 2019, 6, 18. [PubMed: 31179510]
- [95]. a) Haider H, Yang CH, Zheng WJ, Yang JH, Wang MX, Yang S, Zrínyi M, Osada Y, Suo Z, Zhang Q, Zhou J, Chen YM, Soft Matter 2015, 11, 8253; [PubMed: 26350404] b) Caykara T, Yörük D, Demirci S, J. Appl. Polym. Sci 2009, 112, 800;c) Manjua AC, Alves VD, Crespo J. o. G., Portugal CA, ACS Appl. Mater. Interfaces 2019, 11, 21239;d) Zhou Y, Sharma N, Deshmukh

- P, Lakhman RK, Jain M, Kasi RM, J. Am. Chem. Soc 2012, 134, 1630; [PubMed: 22239114] e) Fuhrer R, Athanassiou EK, Luechinger NA, Stark WJ, Small 2009, 5, 383; [PubMed: 19180549] f) Xiong Z, Zheng C, Jin F, Wei R, Zhao Y, Gao X, Xia Y, Dong X, Zheng M, Duan X, Sensors and Actuators B: Chemical 2018, 274, 541;g) Liu Y, Xu K, Chang Q, Darabi MA, Lin B, Zhong W, Xing M, Adv. Mater 2016, 28, 7758. [PubMed: 27417289]
- [96]. a) Satarkar NS, Zhang W, Eitel RE, Hilt JZ, Lab Chip 2009, 9, 1773; [PubMed: 19495462] b) Shen T, Font MG, Jung S, Gabriel ML, Stoykovich MP, Vernerey FJ, Scientific reports 2017, 7, 1. [PubMed: 28127051]
- [97]. Huang H-W, Sakar MS, Petruska AJ, Pané S, Nelson BJ, Nat. Commun 2016, 7, 1.
- [98]. a) Kim SJ, Kim HI, Park SJ, Kim IY, Lee SH, Lee TS, Kim SI, Smart materials and structures 2005, 14, 511;b) Li Y, Sun Y, Xiao Y, Gao G, Liu S, Zhang J, Fu J, ACS Appl. Mater. Interfaces 2016, 8, 26326;c) Migliorini L, Santaniello T, Yan Y, Lenardi C, Milani P, Sensors and Actuators B: Chemical 2016, 228, 758.
- [99]. Takada K, Iida T, Kawanishi Y, Yasui T, Yuchi A, Sensors and Actuators B: Chemical 2011, 160, 1586.
- [100]. Morales D, Palleau E, Dickey MD, Velev OD, Soft Matter 2014, 10, 1337. [PubMed: 24651405]
- [101]. Jiang H, Fan L, Yan S, Li F, Li H, Tang J, Nanoscale 2019, 11, 2231. [PubMed: 30656330]
- [102]. a) Tungkavet T, Seetapan N, Pattavarakorn D, Sirivat A, Polymer 2015, 70, 242;b) Yang C, Liu Z, Chen C, Shi K, Zhang L, Ju X-J, Wang W, Xie R, Chu L-Y, ACS Appl. Mater. Interfaces 2017, 9, 15758;c) Sun Z, Yang L, Zhao J, Song W, J. Electrochem. Soc 2020, 167, 047515.
- [103]. a) Shi J, Guo Z-X, Zhan B, Luo H, Li Y, Zhu D, The Journal of Physical Chemistry B 2005, 109, 14789;b) Ying Z, Wang Q, Xie J, Li B, Lin X, Hui S, J. Mater. Chem. C 2020, 8, 4192.
- [104]. a) Anand SV, Yakut Ali M, Saif MTA, Lab on a Chip 2015, 15, 1879; [PubMed: 25712193] b) Li Z, Seo Y, Aydin O, Elhebeary M, Kamm RD, Kong H, Saif MTA, Proceedings of the National Academy of Sciences 2019, 116, 1543.
- [105]. Feinberg AW, Feigel A, Shevkoplyas SS, Sheehy S, Whitesides GM, Parker KK, Science 2007, 317, 1366. [PubMed: 17823347]
- [106]. a) Shang Y, Chen Z, Fu F, Sun L, Shao C, Jin W, Liu H, Zhao Y, ACS Nano 2019, 13, 796; [PubMed: 30566827] b) Li L, Chen Z, Shao C, Sun L, Sun L, Zhao Y, Adv. Funct. Mater 2020, 30, 1906353;c) Xu B, Han X, Hu Y, Luo Y, Chen CH, Chen Z, Shi P, Small 2019, 15, 1900006.
- [107]. a) Morimoto Y, Onoe H, Takeuchi S, Advanced Robotics 2019, 33, 208;b) Nagamine K, Kawashima T, Sekine S, Ido Y, Kanzaki M, Nishizawa M, Lab on a Chip 2011, 11, 513. [PubMed: 21116545]
- [108]. Wang XQ, Wang CF, Zhou ZF, Chen S, Advanced Optical Materials 2014, 2, 652.
- [109]. Liu T, Liu M, Dou S, Sun J, Cong Z, Jiang C, Du C, Pu X, Hu W, Wang ZL, ACS Nano 2018, 12, 2818. [PubMed: 29494127]
- [110]. Wang S, Li Q, Wang B, Hou Y, Zhang T, Ind. Eng. Chem. Res 2019, 58, 21553.
- [111]. a) Ringer P, Weißl A, Cost A-L, Freikamp A, Sabass B, Mehlich A, Tramier M, Rief M, Grashoff C, Nat. Meth 2017, 14, 1090;b) Cost AL, Khalaji S, Grashoff C, Current protocols in cell biology 2019, 83, e85; [PubMed: 30865383] c) Stabley DR, Jurchenko C, Marshall SS, Salaita KS, Nat. Meth 2012, 9, 64;d) Galior K, Liu Y, Yehl K, Vivek S, Salaita K, Nano Lett. 2016, 16, 341; [PubMed: 26598972] e) Ma VP-Y, Liu Y, Blanchfield L, Su H, Evavold BD, Salaita K, Nano Lett. 2016, 16, 4552. [PubMed: 27192323]
- [112]. Kong HJ, Kim CJ, Huebsch N, Weitz D, Mooney DJ, J. Am. Chem. Soc 2007, 129, 4518. [PubMed: 17381090]
- [113]. He F, You X, Gong H, Yang Y, Bai T, Wang W, Guo W, Liu X, Ye M, ACS Appl. Mater. Interfaces 2020, 12, 6442. [PubMed: 31935061]
- [114]. a) Sun P, Zhang H, Xu D, Wang Z, Wang L, Gao G, Hossain G, Wu J, Wang R, Fu J, Journal of Materials Chemistry B 2019, 7, 2619; [PubMed: 32254994] b) Ma C, Le X, Tang X, He J, Xiao P, Zheng J, Xiao H, Lu W, Zhang J, Huang Y, Adv. Funct. Mater 2016, 26, 8670;c) Cheng Y, Ren K, Yang D, Wei J, Sensors and Actuators B: Chemical 2018, 255, 3117;d) Rivero RE, Molina MA, Rivarola CR, Barbero CA, Sensors and Actuators B: Chemical 2014, 190, 270;e) Chen L, Weng M, Zhou P, Zhang L, Huang Z, Zhang W, Nanoscale 2017, 9, 9825; [PubMed: 28585961] f) Li H, Go G, Ko SY, Park J-O, Park S, Smart Materials and Structures 2016, 25, 027001;g) Han

B, Gao Y-Y, Zhang Y-L, Liu Y-Q, Ma Z-C, Guo Q, Zhu L, Chen Q-D, Sun H-B, Nano Energy 2020, 71, 104578;h) Zhang Y-L, Ma J-N, Liu S, Han D-D, Liu Y-Q, Chen Z-D, Mao J-W, Sun H-B, Nano Energy 2020, 68, 104302;i) Wang T, Li M, Zhang H, Sun Y, Dong B, J. Mater. Chem. C 2018, 6, 6416;j) Li J, Mou L, Zhang R, Sun J, Wang R, An B, Chen H, Inoue K, Ovalle-Robles R, Liu Z, Carbon 2019, 148, 487;k) Qin H, Zhang T, Li N, Cong H-P, Yu S-H, Nat. Commun 2019, 10, 1. [PubMed: 30602773]

- [115]. <https://en.wikipedia.org/wiki/Robot>.
- [116]. a) Wang H, Shi Q, Nakajima M, Takeuchi M, Chen T, Di P, Huang Q, Fukuda T, International Journal of Advanced Robotic Systems 2014, 11, 121;b) Tang J, Yao C, Gu Z, Jung S, Luo D, Yang D, Angew. Chem. Int. Ed 2020, 59, 2490;c) Du X, Cui H, Xu T, Huang C, Wang Y, Zhao Q, Xu Y, Wu X, Adv. Funct. Mater 2020, 30, 1909202;d) Chen Z, Zhao D, Liu B, Nian G, Li X, Yin J, Qu S, Yang W, Adv. Funct. Mater 2019, 29, 1900971;e) Higashi K, Miki N, Sensors and Actuators B: Chemical 2014, 202, 301;f) Morimoto Y, Onoe H, Takeuchi S, Science Robotics 2018, 3;g) Zhang M, Li G, Yang X, Xiao Y, Yang T, Wong T-W, Li T, Smart Materials and Structures 2018, 27, 095016;h) Liang S, Tu Y, Chen Q, Jia W, Wang W, Zhang L, Materials Horizons 2019, 6, 2135.
- [117]. a) Gerboni G, Diodato A, Ciuti G, Cianchetti M, Menciassi A, IEEE/ASME Transactions on Mechatronics 2017, 22, 1881;b) Bilodeau RA, Kramer RK, Frontiers in Robotics and AI 2017, 4, 48;c) Wu Y, Yim JK, Liang J, Shao Z, Qi M, Zhong J, Luo Z, Yan X, Zhang M, Wang X, Science Robotics 2019, 4, eaax1594.
- [118]. a) Galloway KC, Becker KP, Phillips B, Kirby J, Licht S, Tchernov D, Wood RJ, Gruber DF, Soft robotics 2016, 3, 23; [PubMed: 27625917] b) Qin L, Tang Y, Gupta U, Zhu J, Smart Materials and Structures 2018, 27, 045017;c) Joyee EB, Pan Y, Procedia Manufacturing 2019, 34, 566.
- [119]. Polygerinos P, Correll N, Morin SA, Mosadegh B, Onal CD, Petersen K, Cianchetti M, Tolley MT, Shepherd RF, Advanced Engineering Materials 2017, 19, 1700016.
- [120]. D'Eramo L, Chollet B, Leman M, Martwong E, Li M, Geisler H, Dupire J, Kerdraon M, Vergne C, Monti F, Tran Y, Tabeling P, Microsystems & Nanoengineering 2018, 4, 17069.
- [121]. a) Fu G, Zhu Y, Wang W, Zhou M, Li X, ACS Sensors 2019, 4, 2481; [PubMed: 31452364] b) Jadhav AD, Yan B, Luo R-C, Wei L, Zhen X, Chen C-H, Shi P, Biomicrofluidics 2015, 9, 034114.
- [122]. Kwon GH, Choi YY, Park JY, Woo DH, Lee KB, Kim JH, Lee S-H, Lab on a Chip 2010, 10, 1604. [PubMed: 20376390]
- [123]. a) Baldi A, Yuandong G, Loftness PE, Siegel RA, Ziaie B, Journal of Microelectromechanical Systems 2003, 12, 613;b) Park JY, Oh HJ, Kim DJ, Baek JY, Lee SH, Journal of Micromechanics and Microengineering 2006, 16, 656.
- [124]. Lee EL, Von Recum HA, J. Biomed. Mater. Res. Part A 2010, 93, 411.
- [125]. Koike Y, Yokoyama Y, Hayakawa T, Frontiers in Mechanical Engineering 2020, 6.
- [126]. Filippi M, Dasen B, Guerrero J, Garello F, Isu G, Born G, Ehrbar M, Martin I, Scherberich A, Biomaterials 2019, 223, 119468.
- [127]. McKeon-Fischer K, Flagg D, Freeman J, Journal of biomedical materials research Part A 2011, 99, 493. [PubMed: 21913315]
- [128]. Lim JW, Kim H.-j., Kim Y, Shin SG, Cho S, Jung WG, Jeong JH, Polymers 2020, 12, 583.
- [129]. Cezar CA, Roche ET, Vandeburgh HH, Duda GN, Walsh CJ, Mooney DJ, Proceedings of the National Academy of Sciences 2016, 113, 1534.
- [130]. Kirillova A, Maxson R, Stoychev G, Gomillion CT, Ionov L, Adv. Mater 2017, 29, 1703443.
- [131]. van Rijt SH, Bölükbas DA, Argyo C, Datz S, Lindner M, Eickelberg O, Königshoff M, Bein T, Meiners S, ACS Nano 2015, 9, 2377. [PubMed: 25703655]
- [132]. Klumb LA, Horbett TA, Control J. Release 1992, 18, 59.
- [133]. a) Cezar CA, Kennedy SM, Mehta M, Weaver JC, Gu L, Vandeburgh H, Mooney DJ, Adv Healthc Mater 2014, 3, 1869; [PubMed: 24862232] b) Lin F, Zheng J, Guo W, Zhu Z, Wang Z, Dong B, Lin C, Huang B, Lu B, Cellulose 2019, 26, 6861.
- [134]. Kim D.-i., Lee H, Kwon S.-h., Choi H, Park S, Sensors and Actuators B: Chemical 2019, 289, 65.

- [135]. Liang Y, Zhao X, Ma PX, Guo B, Du Y, Han X, Journal of Colloid and Interface Science 2019, 536, 224. [PubMed: 30368094]
- [136]. a) Carrillo-Conde BR, Brewer E, Lowman A, Peppas NA, Industrial & Engineering Chemistry Research 2015, 54, 10197;b) Sung H-W, Sonaje K, Liao Z-X, Hsu L-W, Chuang E-Y, Accounts of Chemical Research 2012, 45, 619. [PubMed: 22236133]
- [137]. Li X, Fu M, Wu J, Zhang C, Deng X, Dhinakar A, Huang W, Qian H, Ge L, Acta biomaterialia 2017, 51, 294. [PubMed: 28069504]
- [138]. del Rio A, Perez-Jimenez R, Liu R, Roca-Cusachs P, Fernandez JM, Sheetz MP, Science 2009, 323, 638. [PubMed: 19179532]
- [139]. Liu C, Kubo K, Wang E, Han K-S, Yang F, Chen G, Escobedo FA, Coates GW, Chen P, Science 2017, 358, 352. [PubMed: 29051377]
- [140]. Su H, Liu Z, Liu Y, Ma VP-Y, Blanchard A, Zhao J, Galior K, Dyer RB, Salaita K, Nano Lett. 2018, 18, 2630. [PubMed: 29589759]

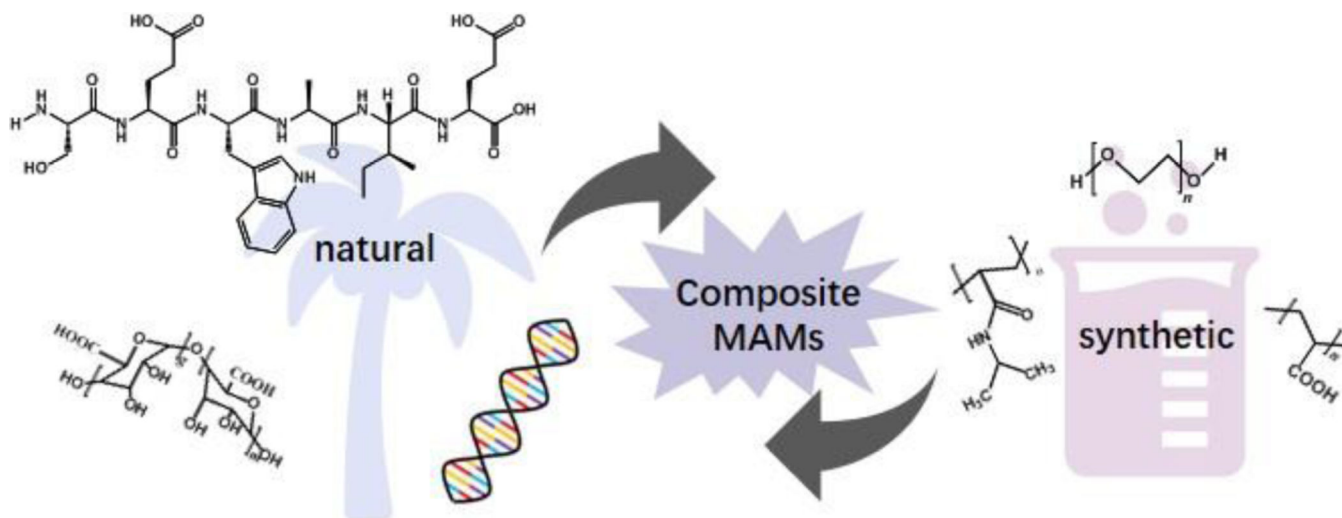


**Figure 1: Schematic of common composition of MAMs.**

There are numerous types of hydrogel polymers that can make up programmable mechanically active materials (MAMs). These include naturally derived polymers, such as alginate polysaccharides, peptide, or deoxyribonucleic acid (DNA) (left), synthetic polymers such as N-isopropylacrylamide (NIPAM) or polyethylene glycol (PEG) (right), or combinations of different polymer types (center).

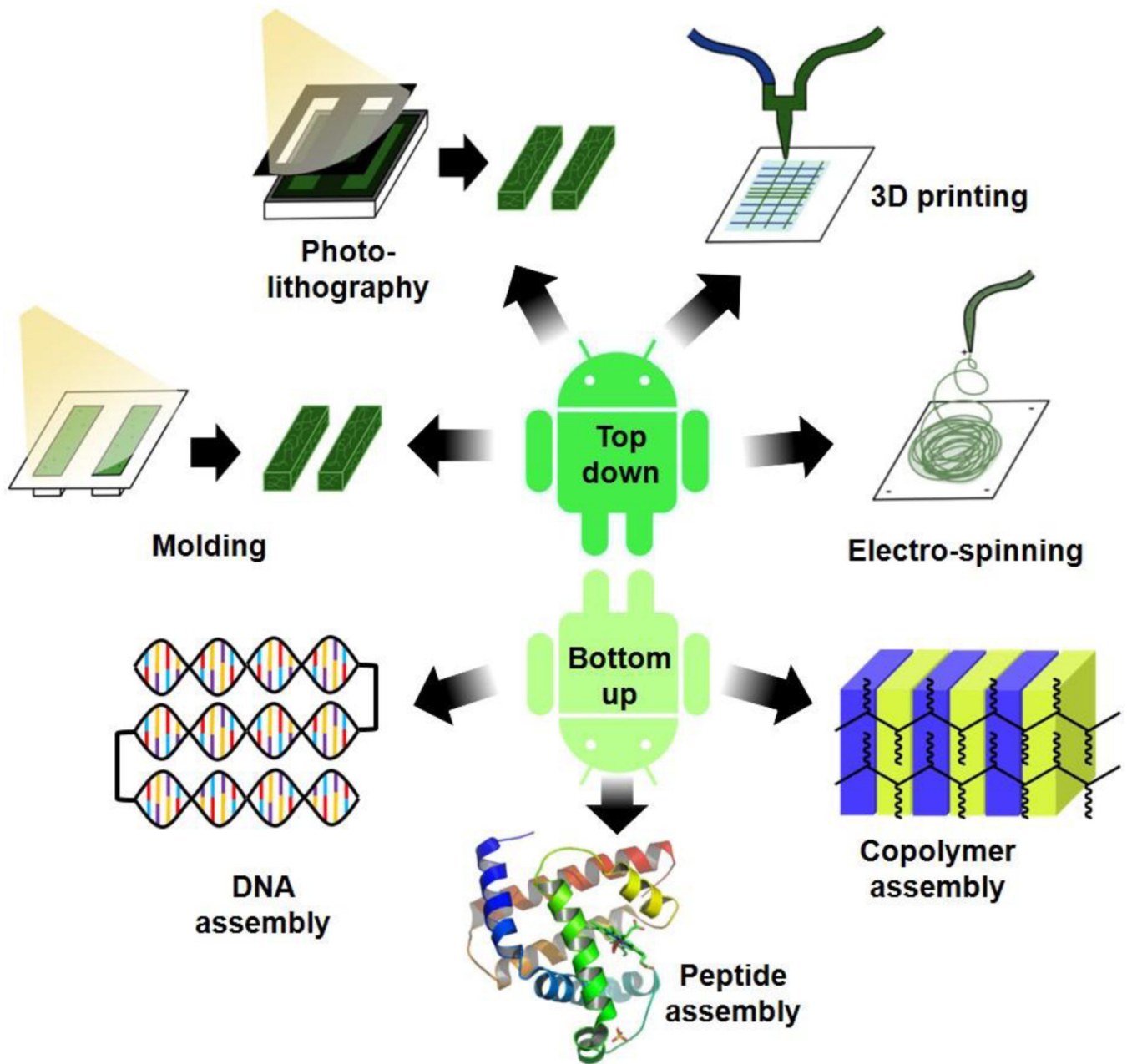


**Figure 2. Schematic of programming hydrogel-based MAMs.**

Numerous techniques are employed in the creation of MAMs to control their design and responsiveness. These are broadly defined as “top-down” techniques that control the material architecture, such as molding, photolithography, additive manufacturing, and electrospinning (top), and “bottom-up” techniques that control the composition of the material, such as DNA self-assembly, peptide sequence engineering, or copolymerization (bottom).

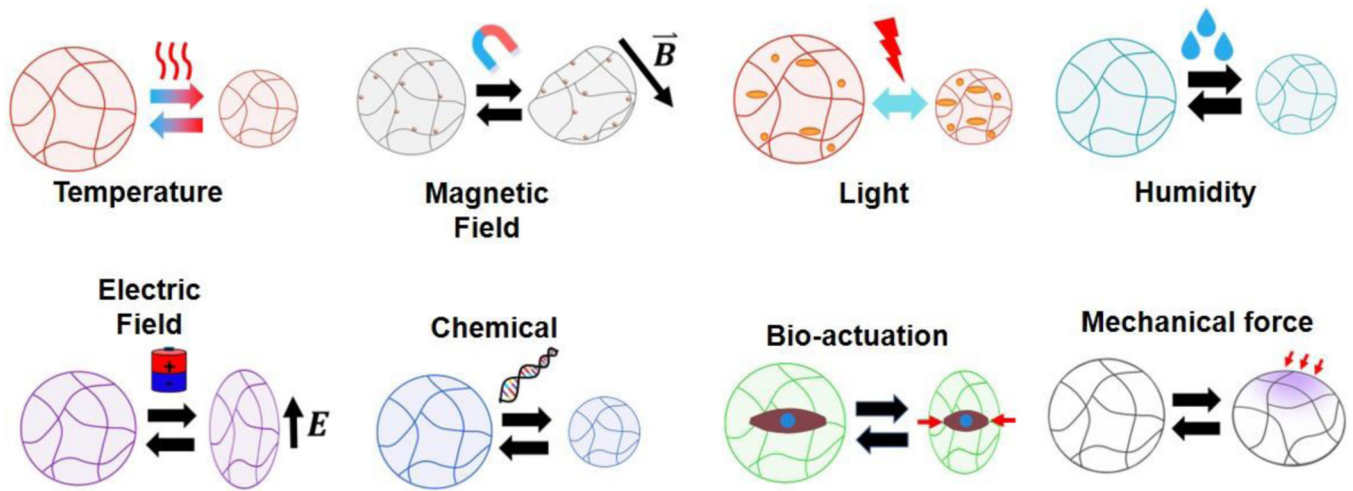


**Figure 3: Schematics of typical responsivities for hydrogel-based MAMs.**

Mechanical actuation in MAMs can be triggered by a variety of stimuli, dependent on the material design. Different MAMs respond to heating, magnetic or electric fields, light, hydration state, oxidation state, specific molecules in solution, pH, ionic strength, and even extrinsic mechanical forces.

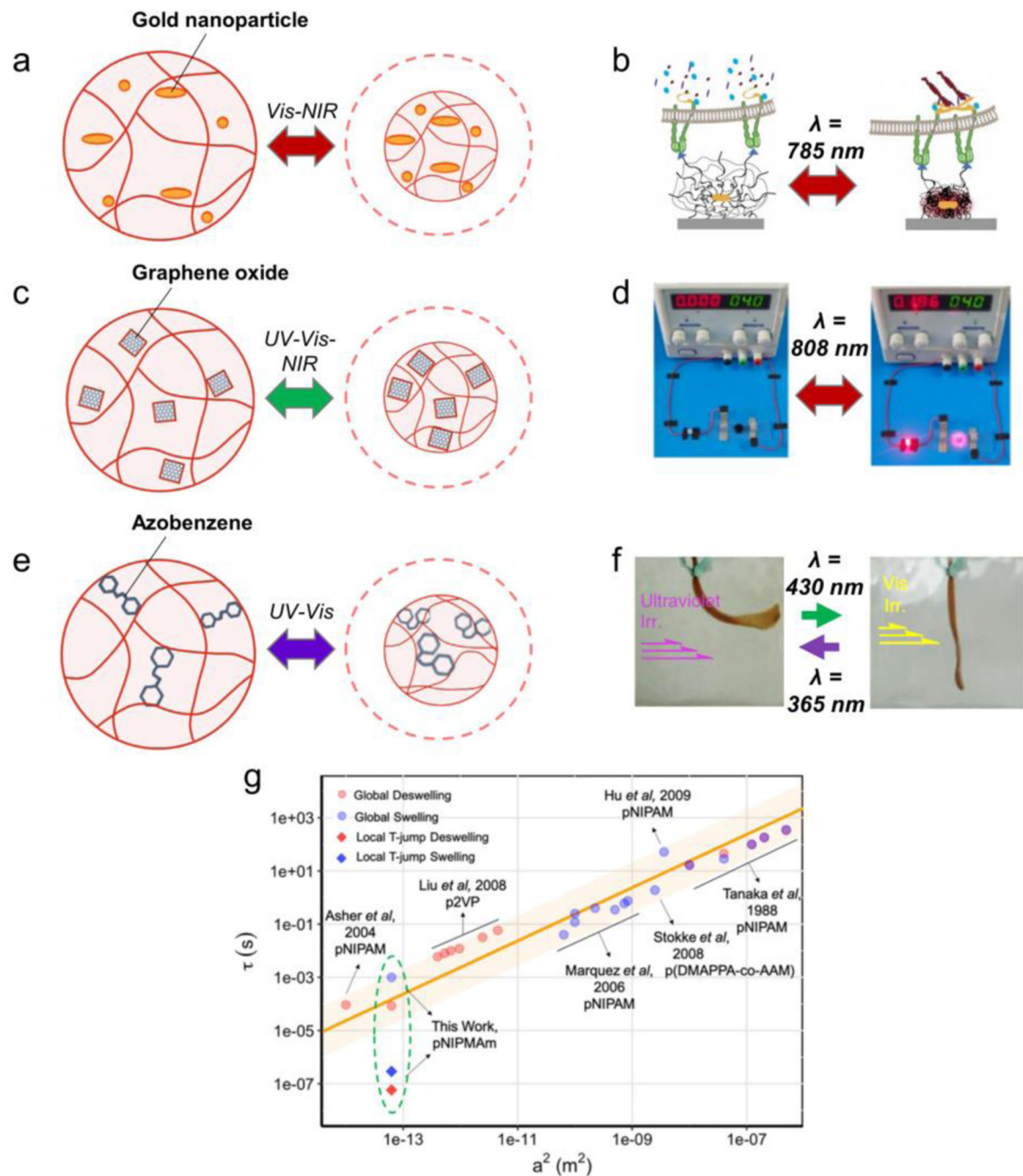


**Figure 4: Mechanisms of photoresponsivity in MAMs.**

Light-responsive MAMs can be designed to be mechanically active under illumination from various wavelengths. a) MAMs made of thermoresponsive polymers with the inclusion of gold nanoparticles is common for inducing IR and visible light responsivity. b) An example of this is the NIPAM-coated gold nanorod structure designed by Liu et al, which was demonstrated to apply forces to cells. Reprinted with permission<sup>[26]</sup>. Copyright 2015, Springer Nature. c) Graphene oxide nanostructures can induce photoresponsivity at a variety of light wavelengths, d) such as one example in which graphene oxide-containing MAMs



were used as an electrical switch controlled by NIR light. Reprinted with permission<sup>[59]</sup>. Copyright 2015, American Chemical Society. e) Responsivity to UV light wavelengths can be programmed by leveraging the photoisomerization of molecules such as azobenzene. f) This can create mechanical actuation in the presence of specific wavelengths, but not others, as demonstrated by Takashima and colleagues. Reprinted with permission<sup>[63b]</sup>. Copyright 2012, Springer Nature. g) Comparison of nanoparticle radius ( $a^2$ ) to actuation time constant ( $\tau$ ) among published thermally and photothermally responsive materials. Reprinted with permission<sup>[68]</sup>. Copyright 2018 American Chemical Society.

Author Manuscript

Author Manuscript

Author Manuscript

Author Manuscript

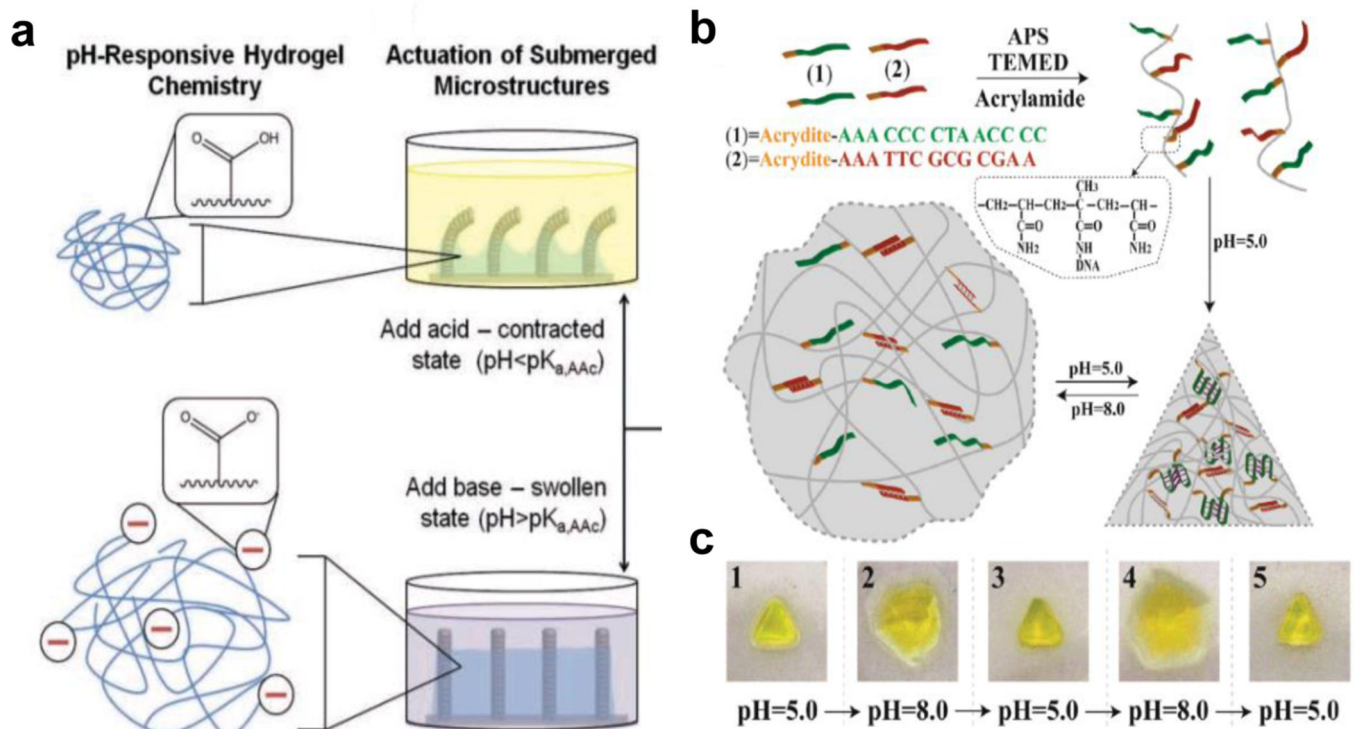


**Figure 5. pH responsive MAMs.**

a) A chip designed with polymer microstructures that is surrounded by a responsive hydrogel matrix. Micropillars on the chip deform in response to pH changes sensed by the responsive hydrogel, driving the actuation mechanism. Reproduced with permission<sup>[69b]</sup>. Copyright 2011, Wiley-VCH. b) DNA hydrogel-based MAMs that have shape memory function in respond to different pH conditions. Decreased pH causes restructuring of the DNA base paring, resulting in deformation of the bulk gel. c) This effect is demonstrated to be highly reversible and repeatable. Reproduced with permission<sup>[75b]</sup>. Copyright 2015, Wiley-VCH.

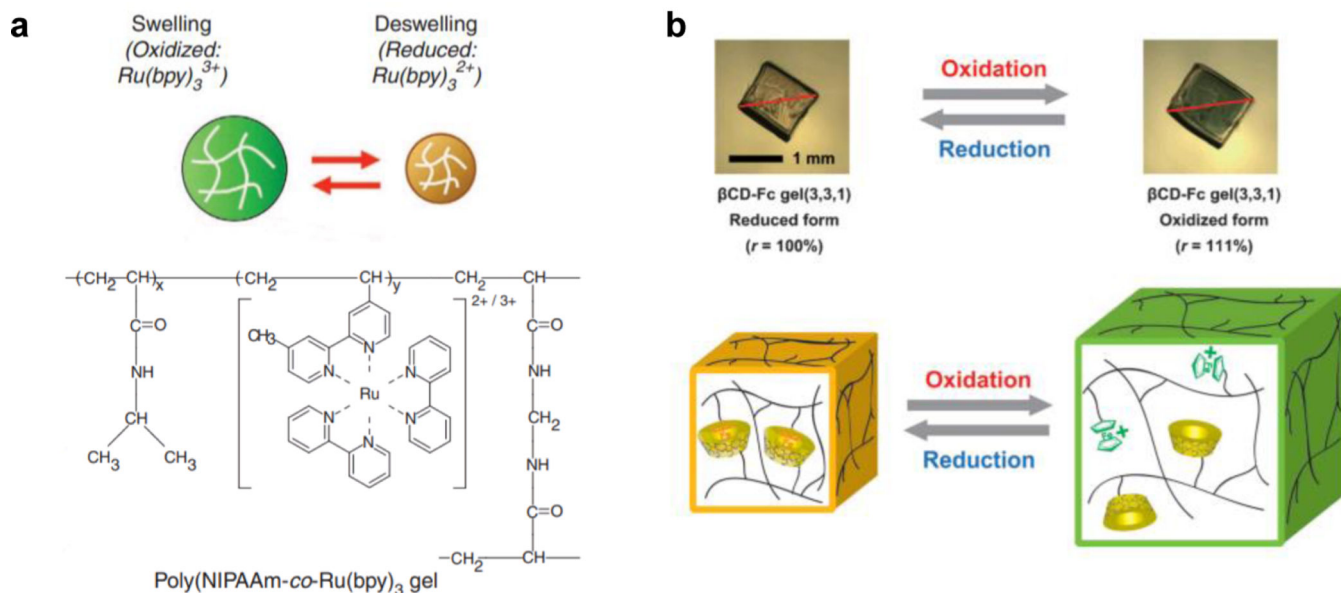


**Figure 6. MAMs with chemical-induced redox responsivity.**

a) A schematic of the Belousov–Zhabotinsky (BZ) reaction, in which oxidation and reduction of ruthenium tris(2,2'-bipyridine) changes hydrogel hydrophilicity to swell and deswell the MAM. driven MAMs. Readapted with permission<sup>[77]</sup>. Copyright 2014, Springer Nature. b) A schematic of a MAM with host-guest interactions between ferrocene and  $\beta$ -cyclo-dextrin ( $\beta$ CD) in the hydrogel network. The cavity of  $\beta$ CD has better accommodation to reduced form of ferrocene, causing shrinkage of the gel as ferrocene- and  $\beta$ CD-modified hydrogel strands are drawn together through this interaction. Readapted with permission<sup>[76c]</sup>. Copyright 2013, Wiley-VCH.

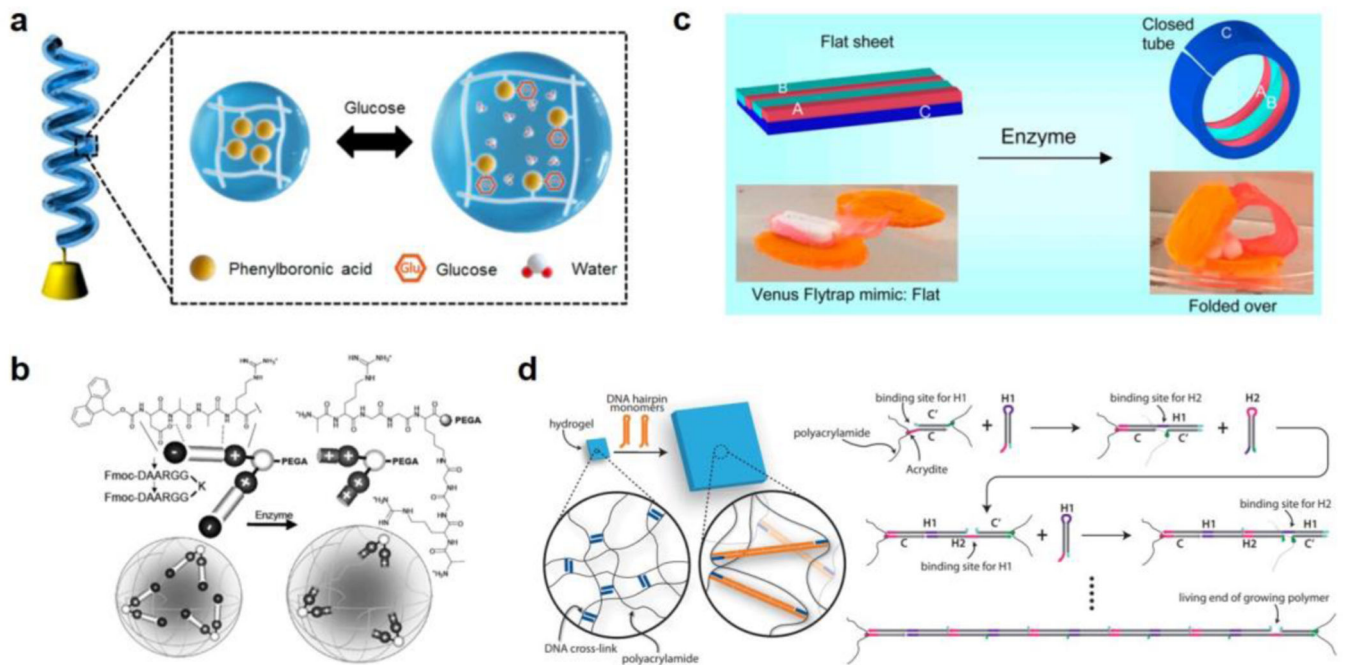


**Figure 7. Biomolecule-responsive MAMs.**

a) A glucose responsive MAM, comprised of a self-helical hydrogel fiber modified with phenylboronic acid groups that are repelled from each other in the presence of glucose. Readapted with permission<sup>[83a]</sup>. Copyright 2020, American Chemical Society. b) An enzymatically actuated MAM, in which enzyme cleavage removes charge shielding groups and causes electrostatic repulsion within the polymer network, causing gel swelling. Readapted with permission<sup>[84a]</sup>. Copyright 2009, Royal Society of Chemistry. c) A structurally programmed MAM with large amplitude of enzymatic response that induces curvature to the material in the presence of an enzyme, due to the multilayered structure of the MAM. Readapted with permission<sup>[84c]</sup>. Copyright 2016, American Chemical Society. d) A sequence-specific DNA-responsive MAM, in which the presence of a specific target strand triggers a hybridization chain reaction resulting in large volume changes in the gel. Readapted with permission<sup>[23]</sup>. Copyright 2017, American Association for the Advancement of Science.

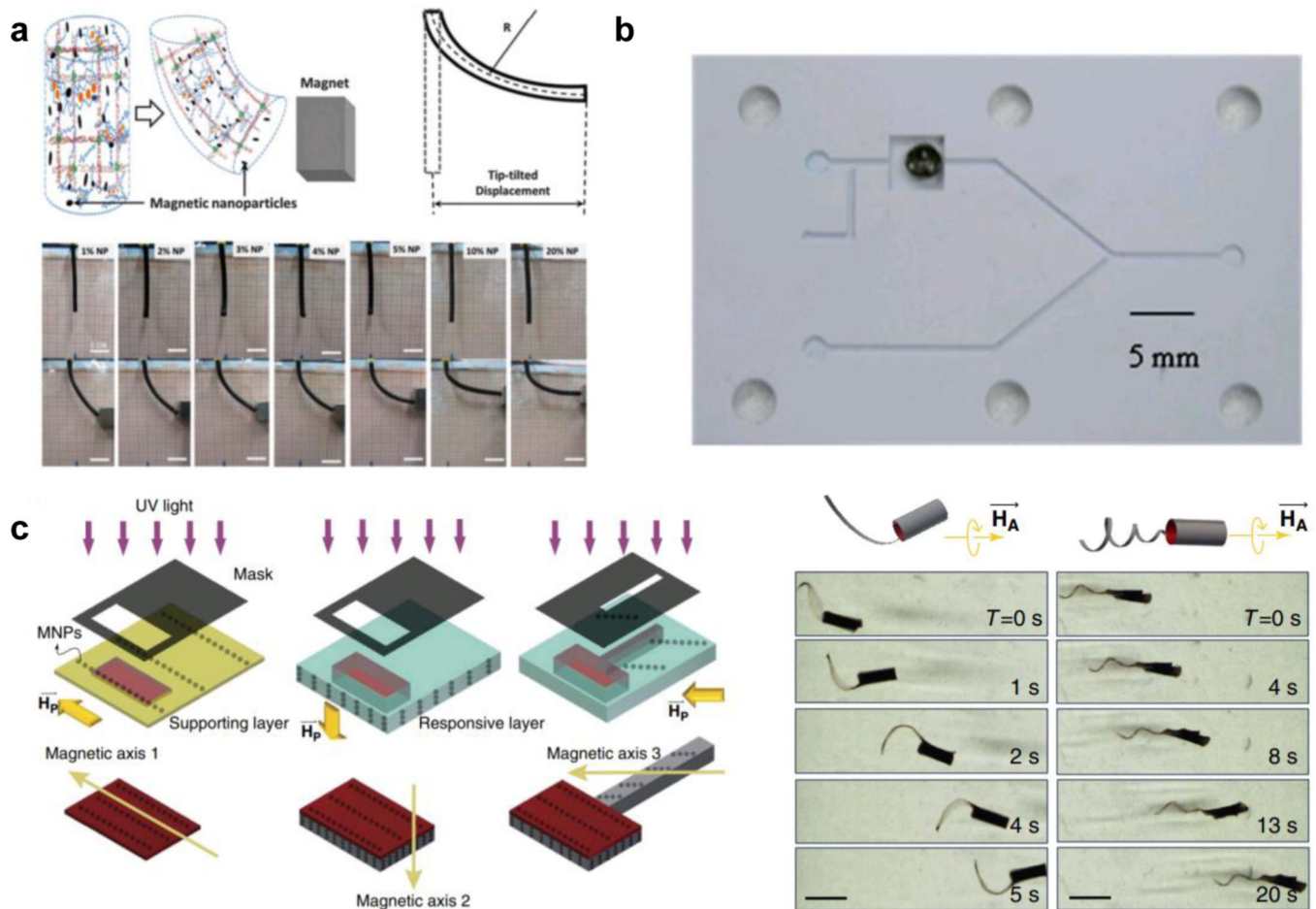


**Figure 8. Magnetic field responsive MAMs.**

a) Polyacrylamide hydrogel MAMs embedded with randomly distributed MNPs. This material shows a very strong response, bending in the direction of an applied magnetic field even at low MNP contents. Readapted with permission<sup>[95a]</sup>. Copyright 2015, Royal Society of Chemistry. b)  $\text{Fe}_3\text{O}_4/\text{pNIPAM}$  composite (black dot) that can open/close a microfluidic channel upon the application of alternating magnetic field. This field heats the iron oxide particles, causing the deswelling of the pNIPAM polymer that opens the channel. Readapted with permission<sup>[96a]</sup>. Copyright 2009 Royal Society of Chemistry. c) (left) Magnetic responsive MAMs can also be fabricated with pre-organized MNPs. This induces sensitivity to the orientation of an applied magnetic field (right), resulting in a highly sensitive and controllable soft robot. Readapted with permission<sup>[97]</sup>, Copyright 2016, Springer Nature.

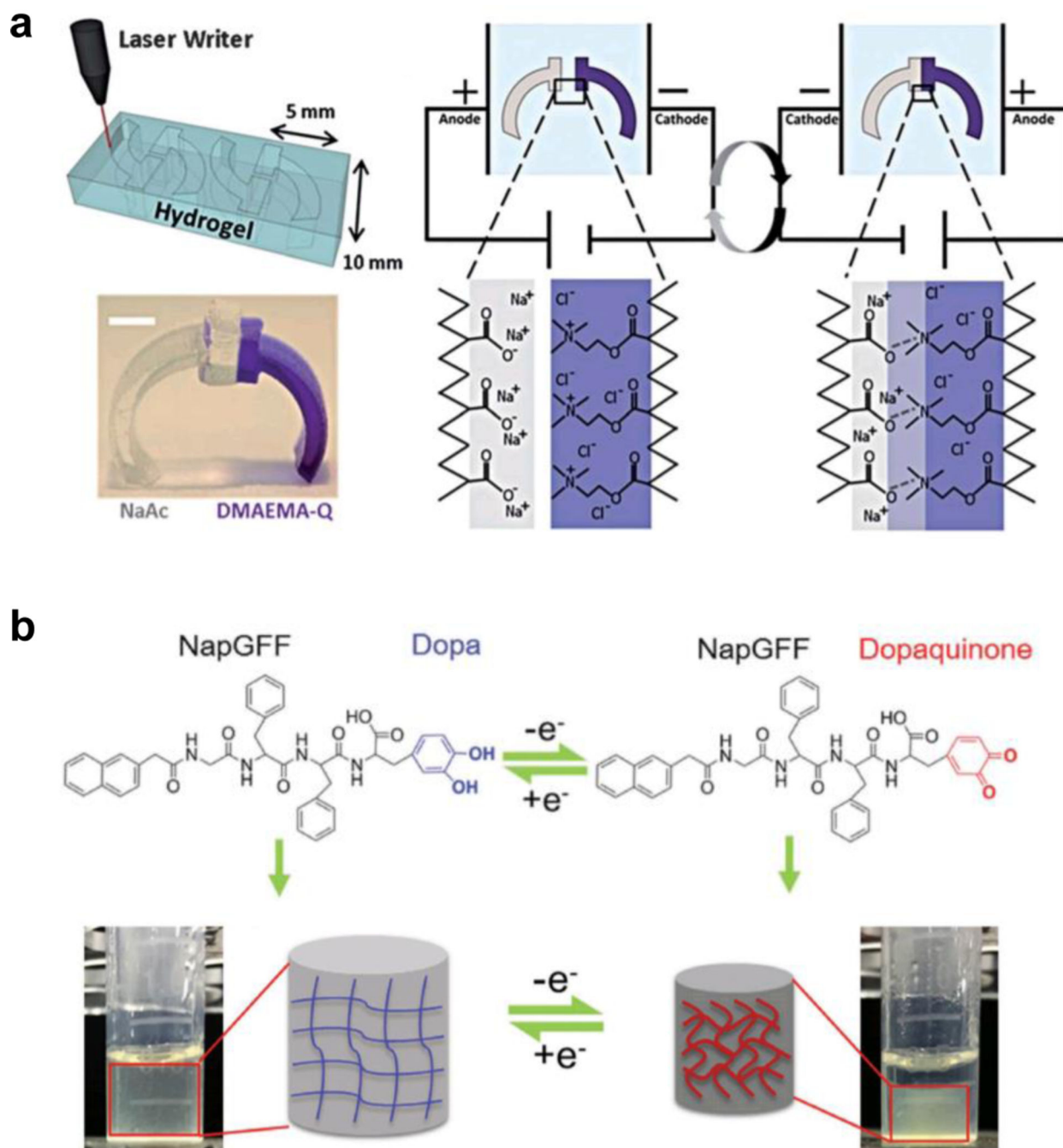


**Figure 9. Electrical field responsive MAMs.**

a) A two “leg” self-walking EFRMAM, fabricated using top-down design, with different “legs” that respond to electrical field direction, resulting in locomotion. Readapted with permission<sup>[100]</sup>. Copyright 2014, Royal Society of Chemistry. b) Structure and function of dopa-based MAMs, in electrical power induces a redox reaction that deswells the hydrogel. Readapted with permission<sup>[25]</sup>. Copyright 2016, Wiley VCH.

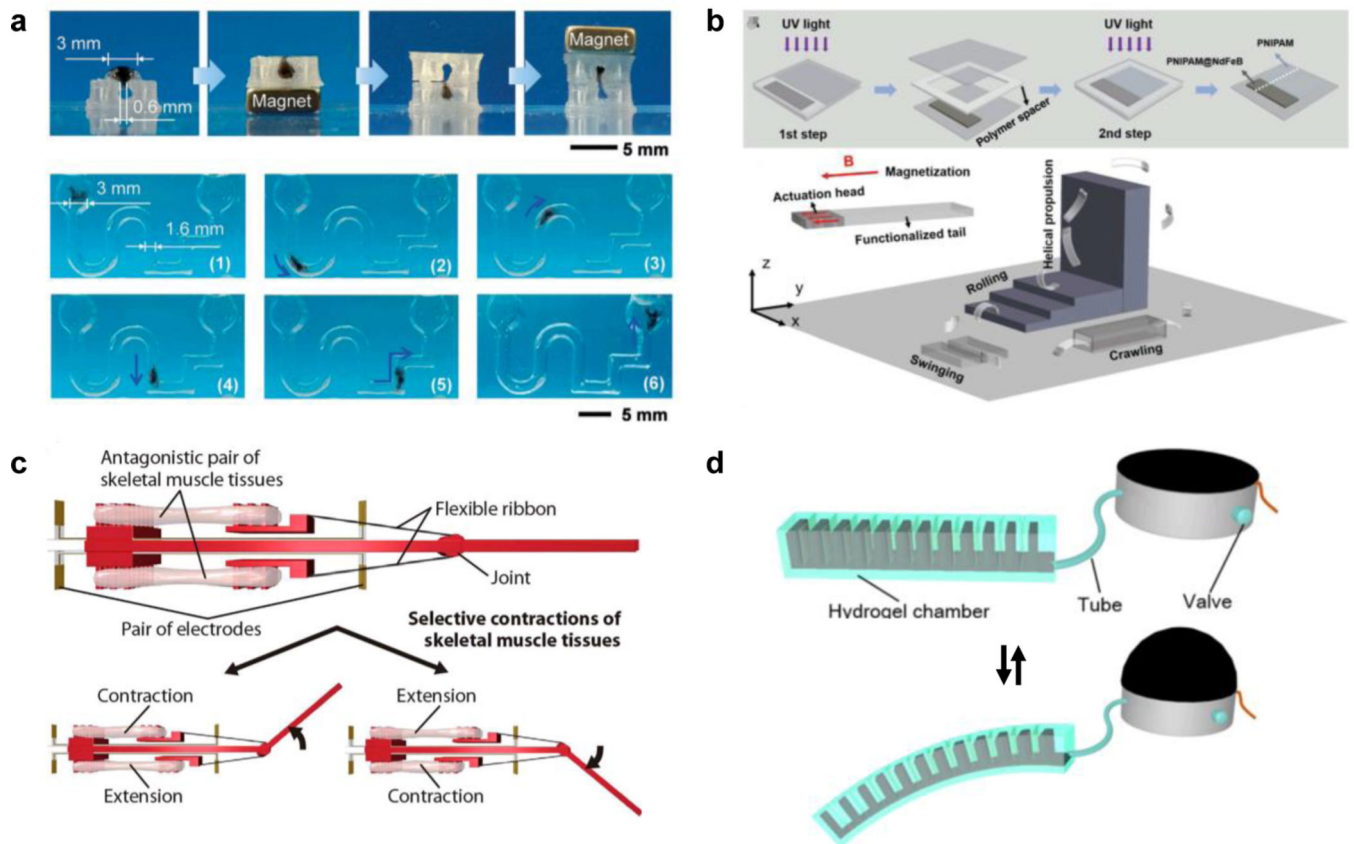


**Figure 10. Robotic MAMs with different actuating mechanisms.**

a) An example of a paramagnetic DNA hydrogel soft robot with magnetic field-driven navigation of its locomotion. Readapted with permission<sup>[116b]</sup>. Copyright 2020, Wiley-VCH. b) A ferromagnetic hydrogel MAMs embedded with NdFeB particles. The MAM is pre-magnetized during fabrication to develop the ferromagnetic response, resulting in a more sophisticated moving behavior of the soft robot under a magnetic field. Readapted with permission<sup>[116c]</sup>. Copyright 2020, Wiley-VCH. c) A bio-actuated MAM comprised of a muscle cell-laden Matrigel scaffold. Actuation of this MAM is activated by applying electrical stimulation with embedded gold electrodes, triggering contraction of the cells. Readapted with permission<sup>[116f]</sup>. Copyright 2018, American Association for the Advancement of Science. d) A hydrogel MAM robot designed with asymmetrical cavities that change shape under varying hydraulic pressure, resulting in material bending. Readapted with permission<sup>[116g]</sup>. Copyright 2018, IOP publishing.

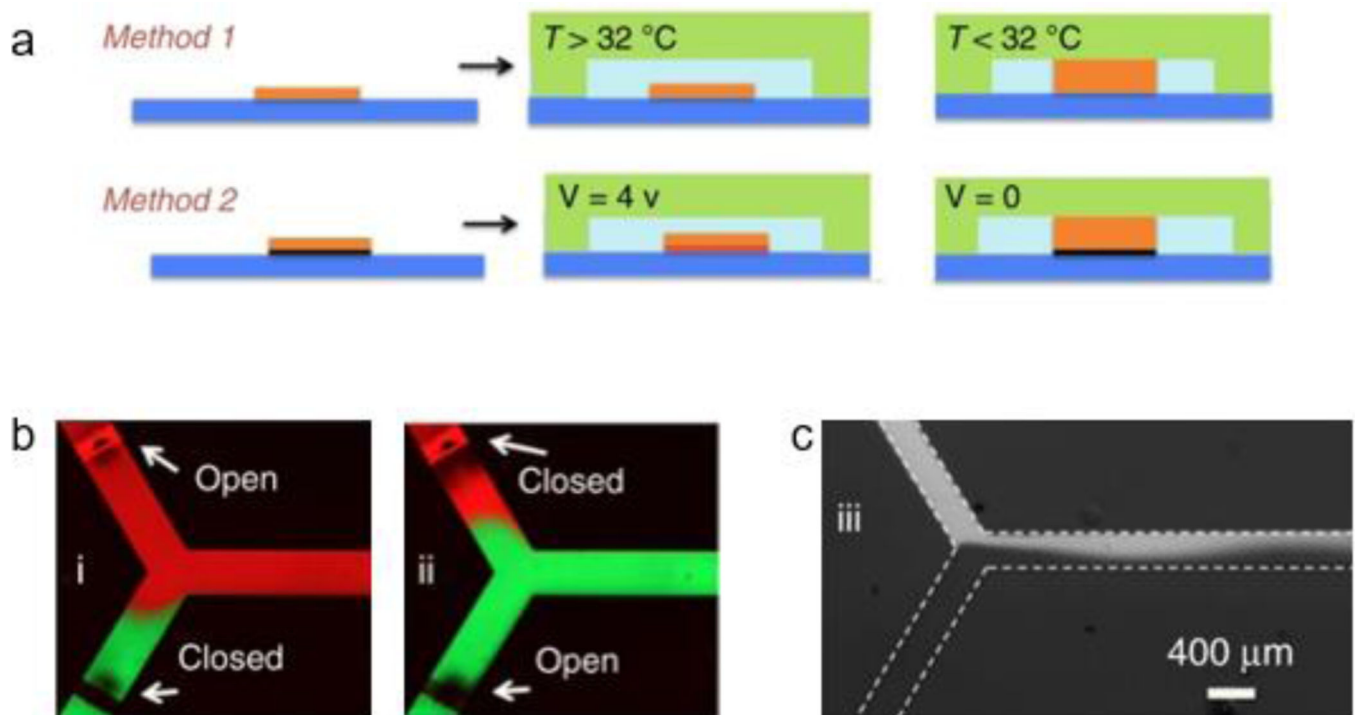


**Figure 11: MAMs for microfluidic control.**

MAMs have been recently studied for their use as valves for microfluidic devices. a) Two mechanisms that have been studied in this application are thermo-responsivity (top) and electro-responsivity (bottom). In this work, these stimulation mechanisms both work by shrinking a MAM valve that blocks the microfluidic channel, allowing fluid to pass. b) The efficacy of these valves is demonstrated through the control of flow of colored liquid, where closing and opening alternating channels results in a complete change of the color flowing through the main channel with little mixing observed. c) Alternating opening and closing of upper and lower channels twice per second demonstrates rapid response of the MAM valves, as evidenced by changing amounts of fluorescently labeled (light) and unlabeled (dark) liquid in the main channel of the device. Reproduced with permission<sup>[120]</sup>. Copyright 2018, Springer-Nature.



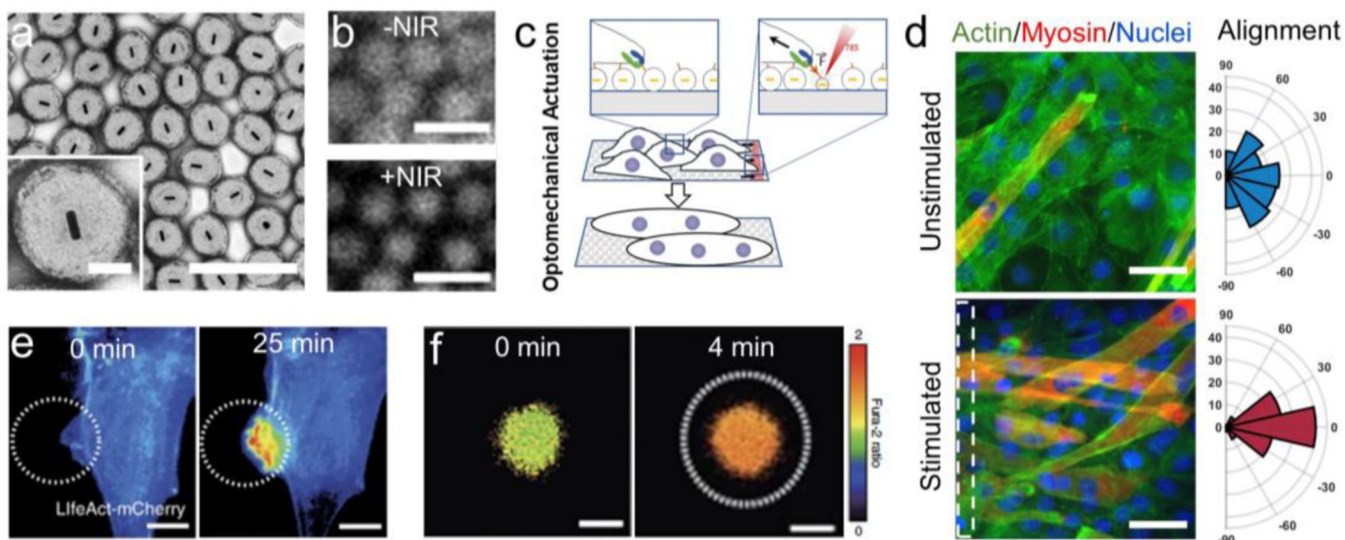


**Figure 12: Photoresponsive MAMs direct cell behavior.**

a) Optomechanical actuators (OMAs, as described in Section 4.2.1) are gold-pNIPMAM composite nanoparticles that contract when exposed to NIR light. TEM image, scale bar = 1  $\mu\text{m}$ , inset scale bar = 200 nm. b) Fluorescent labeling of OMA provides evidence particle collapse when exposed to NIR light. Scale bar = 1  $\mu\text{m}$ . c) These MAMs can be modified to facilitate cell attachment, applying force with high spatial precision to study the role of mechanics in cell activity across a variety of cell types. d) Repeated stimulation of myoblasts over 5 days enhanced markers of maturation (left), such as myosin expression (red) and multinucleation (nuclei, blue), as well as cellular alignment (actin, green; histograms, right). Scale bar = 50  $\mu\text{m}$ . e) Fibroblast cells responded to short-term mechanical stimulation by extending in the direction of the stimulus, and increasing actin polymerization. Scale bar = 10  $\mu\text{m}$ . f) Mechanical stimulation of T cells was able to significantly enhance Fura-2 calcium signaling, an important marker of T cell activation. Scale bar = 5  $\mu\text{m}$ . Figures readapted with permission from: a, c-d) Ramey-Ward et al. (2020) *ACS Appl. Mat. Inter.* Copyright 2020 American Chemical Society [57]; b,e-f) Liu et al. (2016) *Nat. Meth.* Copyright 2016 Springer-Nature [26].

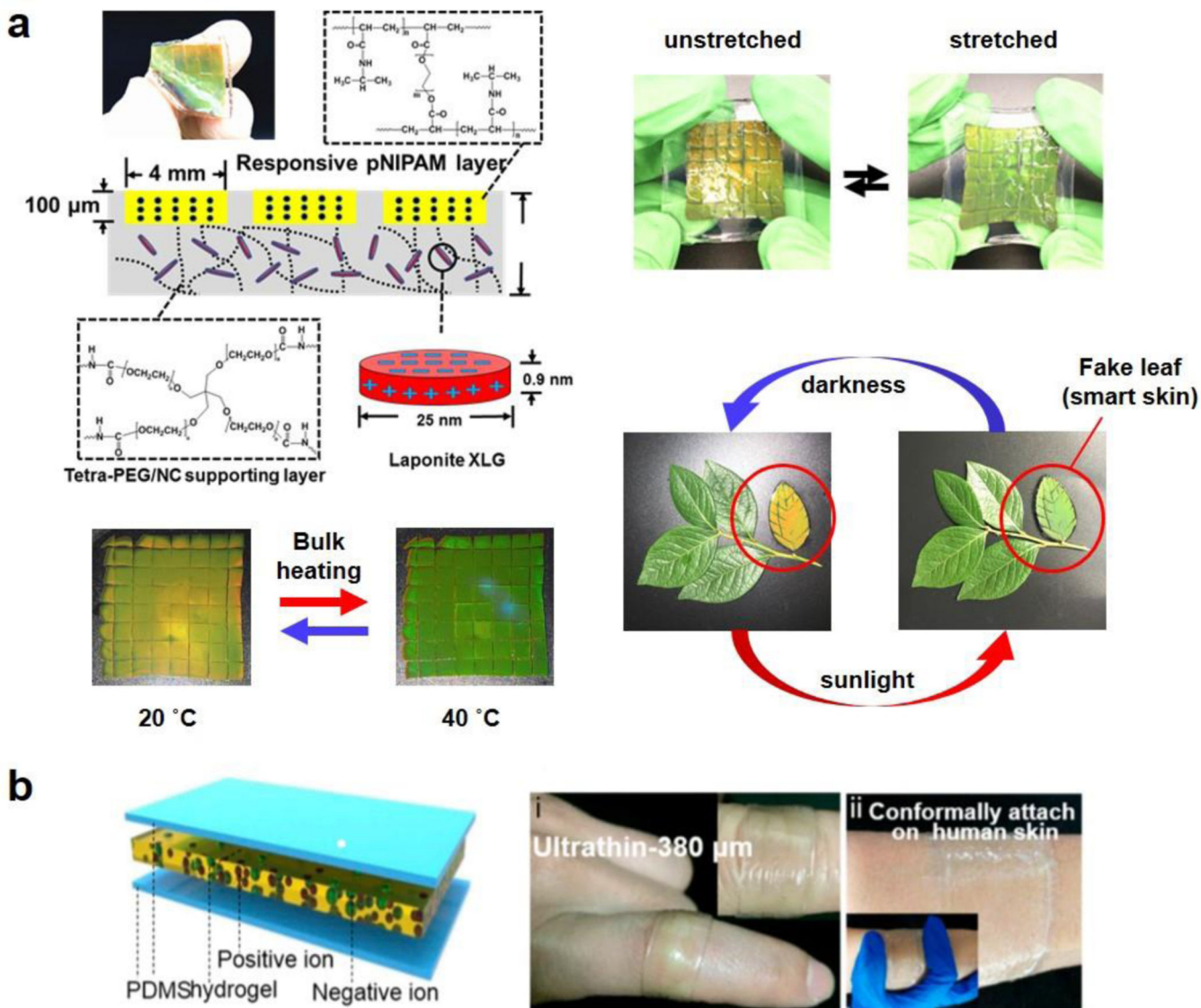


**Figure 13. Smart skin MAMs.**

a) (top left) NIPAM hydrogels containing photonic crystals were embedded into a strain-accommodating material, with tunable toughness via the inclusion of Laponite nanoclay particles. This created a color changing smart skin that maintains its shape and size during its sensing. This strain-accommodating smart skin can change its color in response to (bottom left) bulk heating, (top right) stretching, and (bottom right) sunlight. Such a material holds potential applications for solar-triggered camouflage, as evidenced by its visual similarity to natural foliage. Readapted with permission<sup>[34]</sup>. Copyright 2019, American Chemical Society. b) A triboelectric energy-harvesting skin that can sense the mechanical force and transfer the energy into electrical power. (left) A schematic of the MAM, showing the PDMS electrode layers (blue) and dielectric polymer hydrogel core (yellow). (right) Demonstration of these thin and compliant smart skins that can be conformally attach on human skin. Readapted with permission<sup>[109]</sup>. Copyright 2018, American Chemical Society.

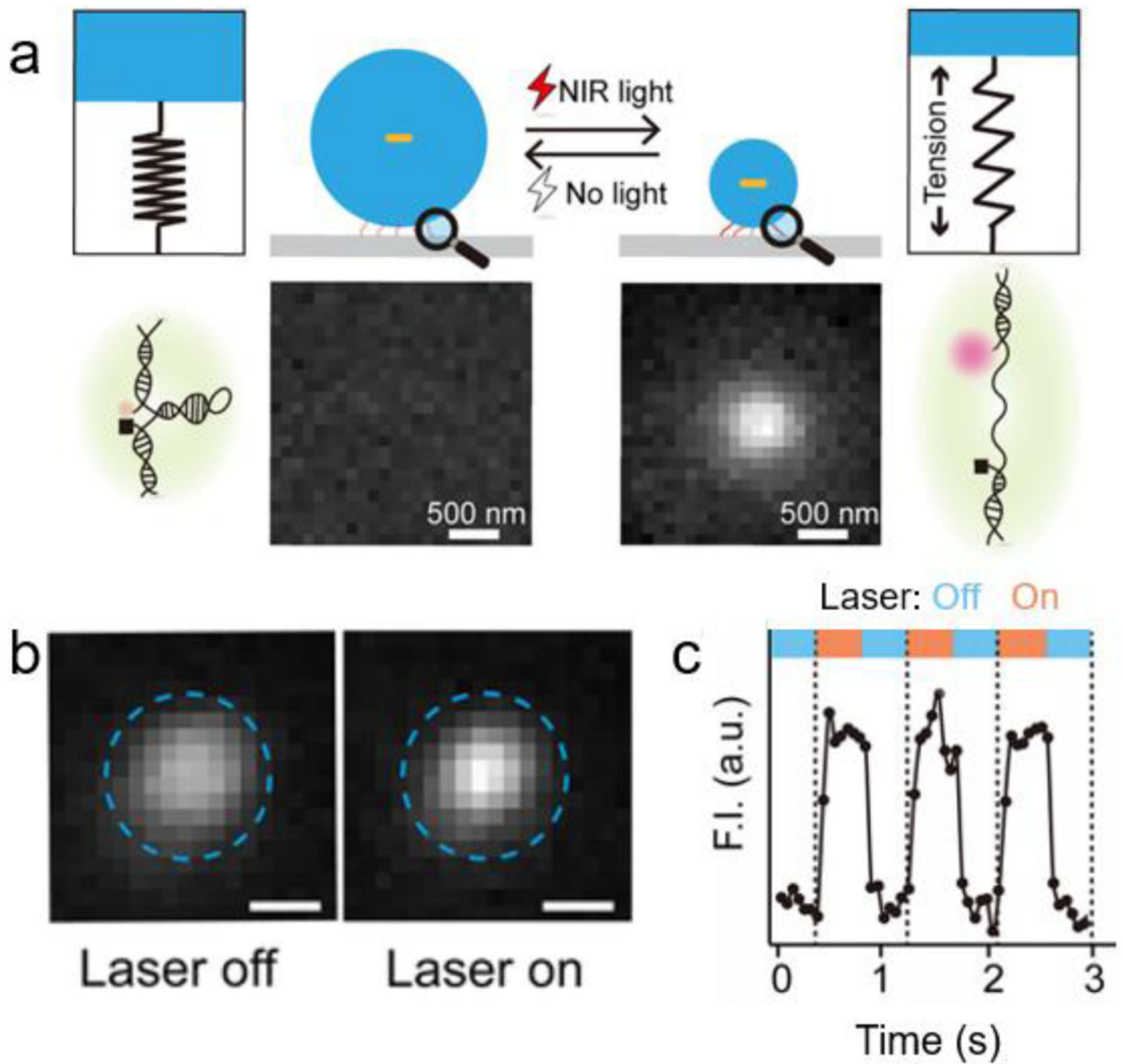


**Figure 14. MAMs for single molecule force spectroscopy.**

a) (top middle) Schematic of the polymer force clamp (PFC), a composite MAM nanoparticle capable of delivering pN-scale forces to attached biomolecules through NIR illumination. Much like stretching a spring, (bottom) the actuation of PFC MAMs unfolds fluorescently labeled DNA molecules, resulting in increased fluorescence. b) Actuation of PFCs was evidenced through fluorescent labeling of the MAM, with increased fluorescence density under NIR illumination indicating particle shrinkage. c) PFCs provide robust and repeatable unfolding of attached biomolecules, shown by cyclic increases in fluorescence

from unfolded DNA structures across multiple NIR laser exposures. Reproduced with permission.<sup>[140]</sup> Copyright 2018, American Chemical Society.

Author Manuscript

Author Manuscript

Author Manuscript

Author Manuscript

**Table 1:**

Comparison of several MAMs examples with different compositions

Composition	Responsivity	Modulus (MPa)	Actuation Magnitude	Actuation Speed	Reference
Acrylamide-phenylboric acid	Biomolecule (glucose)	0.56–0.73	L = 2.3%	1 h	Sim [78a]
Polyacrylamide-alginate	Magnetic (Fe <sub>3</sub> O <sub>4</sub> )	0.2	k = 0.2/cm	---	Haider [90a]
Poly-L-lysine	Redox	---	V = 97%	380 s	Wang [71d]
Alginate-dimethyl acrylamide	Chemical (ion)	0.02–0.05	V = 40%	48 m	Athas [79c]
Acrylic acid-co-acrylamide	Chemical (salt)	0.52–0.8	L = 1.5–24.4%	1 m	Zhen [4a]
PEG-DA	Chemical (humidity)	0.25	k = 0.4/cm	4–10 s	Lv [12,83]
Alginate	Chemical (salt)	---	V > 50%	0.5–3 m	Moe [13a]
DNA	Multiple	---	V = 76%	30–60 m	Zhao [29a]
DNA	Multiple	0.002	V = 100x	25 h	Cangialosi [23]
NIPAM-graphene oxide	Light (NIR)	0.05	V = 90%	5–15 m	Shi [55]

The design of MAMs involves the consideration of several factors, such as material properties and degree of strain applied, dependent on the desired outcomes and applications. Here, several examples of synthetic polymers (red), naturally derived polymers (blue), and composites of the two (purple) exhibiting a variety of responsive mechanisms are compared to show a range of potential parameters. Material modulus is given in MPa. Actuation magnitude is given as either length change ( L ), volume change ( V ), or bending curvature ( $k=(\pi/180)*(\theta_{\text{bend}}/\text{length})$ ). Actuation speed is the time to achieve the reported actuation magnitude.